CHAPTER **4**

The Potential for Abrupt Change in the Atlantic Meridional Overturning Circulation

Lead Author: **Thomas L. Delworth**,* NOAA Geophysical Fluid Dynamics Laboratory

Contributing Authors: **Peter U. Clark**,* Department of Geosciences, Oregon State University

Marika Holland, National Center for Atmospheric Research

William E. Johns, Rosenstiel School of Marine and Atmospheric Science, University of Miami

Till Kuhlbrodt, Department of Meteorology, NCAS-Climate, University of Reading, United Kingdom

Jean Lynch-Stieglitz, School of Earth and Atmospheric Sciences, Georgia Institute of Technology

Carrie Morrill,* Cooperative Institute for Research in Environmental Sciences, University of Colorado, and NOAA National Climatic Data Center

Richard Seager,* Lamont-Doherty Earth Observatory, Columbia University

Andrew J. Weaver,* School of Earth and Ocean Sciences, University of Victoria, Canada

Rong Zhang, NOAA Geophysical Fluid Dynamics Laboratory

———
* SAP 3.4 Federal Advisory Committee member

KEY FINDINGS

The Atlantic Meridional Overturning Circulation (AMOC) is an important component of the Earth's climate system, characterized by a northward flow of warm, salty water in the upper layers of the Atlantic, and a southward flow of colder water in the deep Atlantic. This ocean circulation system transports a substantial amount of heat from the Tropics and Southern Hemisphere toward the North Atlantic, where the heat is transferred to the atmosphere. Changes in this circulation have a profound impact on the global climate system, as indicated by paleoclimate records. These include, for example, changes in African and Indian monsoon rainfall, atmospheric circulation of relevance to hurricanes, and climate over North America and Western Europe. In this chapter, we have assessed what we know about the AMOC and the likelihood of future changes in the AMOC in response to increasing greenhouse gases, including the possibility of abrupt change. We have five primary findings:

- It is very likely that the strength of the AMOC will decrease over the course of the 21st century in response to increasing greenhouse gases, with a best estimate decrease of 25–30%.

- Even with the projected moderate AMOC weakening, it is still very likely that on multidecadal to century time scales a warming trend will occur over most of the European region downstream of the North Atlantic Current in response to increasing greenhouse gases, as well as over North America.

- No current comprehensive climate model projects that the AMOC will abruptly weaken or collapse in the 21st century. We therefore conclude that such an event is very unlikely. Further, an abrupt collapse of the AMOC would require either a sensitivity of the AMOC to forcing that is far greater than current models suggest or a forcing that greatly exceeds even the most aggressive of current projections (such as extremely rapid melting of the Greenland ice sheet). However, we cannot completely exclude either possibility.

- We further conclude it is unlikely that the AMOC will collapse beyond the end of the 21st century because of global warming, although the possibility cannot be entirely excluded.

- Although our current understanding suggests it is very unlikely that the AMOC will collapse in the 21st century, the potential consequences of such an event could be severe. These would likely include sea level rise around the North Atlantic of up to 80 centimeters (in addition to what would be expected from broad-scale warming of the global ocean and changes in land-based ice sheets due to rising CO_2), changes in atmospheric circulation conditions that influence hurricane activity, a southward shift of tropical rainfall belts with resulting agricultural impacts, and disruptions to marine ecosystems.

The above conclusions depend upon our understanding of the climate system, and on the ability of current models to simulate the climate system. However, these models are not perfect, and the uncertainties associated with these models form important caveats to our conclusions. These uncertainties argue for a strong research effort to develop the observations, understanding, and models required to predict more confidently the future evolution of the AMOC.

CHAPTER 4. RECOMMENDATIONS

We recommend the following activities to advance both our understanding of the AMOC and our ability to predict its future evolution:

- Improve long-term monitoring of the AMOC. This monitoring would likely include observations of key processes involved in deep water formation in the Labrador and Norwegian Seas, and their communication with the rest of the Atlantic (such as the Nordic Sea inflow, and overflow across the Iceland-Scotland Ridge), along with observing the more complete three-dimensional structure of the AMOC, including sea surface height. Such a system needs to be in place for decades to properly characterize and monitor the AMOC.

- Improve understanding of past AMOC changes through the collection and analysis of those proxy records that most effectively document AMOC changes and their impacts in past climates (hundreds to many thousands of years ago). Among these proxy records are geochemical tracers of water masses such as $\delta^{13}C$ and dynamic tracers that constrain rates of the overturning circulation such as the protactinium/thorium (Pa/Th) proxy. These records provide important insights on how the AMOC behaved in substantially different climatic conditions and thus greatly facilitate our understanding of the AMOC and how it may change in the future.

- Accelerated development of climate system models incorporating improved physics and resolution, and the ability to satisfactorily represent small-scale processes that are important to the AMOC. This would include the addition of models of land-based ice sheets and their interactions with the global climate system.

- Increased emphasis on improved theoretical understanding of the processes controlling the AMOC, including its inherent variability and stability, especially with respect to climate change. Among these important processes are the role of small-scale eddies, flows over sills, mixing processes, boundary currents, and deep convection. In addition, factors controlling the large-scale water balance are crucial, such as atmospheric water-vapor transport, precipitation, evaporation, river discharge, and freshwater transports in and out of the Atlantic. Progress will likely be accomplished through studies combining models, observational results, and paleoclimate proxy evidence.

- Development of a system to more confidently predict the future behavior of the AMOC and the risk of an abrupt change. Such a prediction system should include advanced computer models, systems to start model predictions from the observed climate state, and projections of future changes in greenhouse gases and other agents that affect the Earth's energy balance. Although our current understanding suggests it is very unlikely that the AMOC will collapse in the 21st century, this assessment still implies up to a 10% chance of such an occurrence. The potentially severe consequences of such an event, even if very unlikely, argue for the rapid development of such a predictive system.

1. INTRODUCTION

The oceans play a crucial role in the climate system. Ocean currents move substantial amounts of heat, most prominently from lower latitudes, where heat is absorbed by the upper ocean, to higher latitudes, where heat is released to the atmosphere. This poleward transport of heat is a fundamental driver of the climate system and has crucial impacts on the distribution of climate as we know it today. Variations in the poleward transport of heat by the oceans have the potential to make significant changes in the climate system on a variety of space and time scales. In addition to transporting heat, the oceans have the capacity to store vast amounts of heat. On the seasonal time scale, this heat storage and release has an obvious climatic impact, delaying peak seasonal warmth over some continental regions by a month after the summer solstice. On longer time scales, the ocean absorbs and stores most of the extra heating that comes from increasing greenhouse gases (Levitus *et al.,* 2001), thereby delaying the full warming of the atmosphere that will occur in response to increasing greenhouse gases.

One of the most prominent ocean circulation systems is the Atlantic Meridional Overturning Circulation (AMOC). As described in subsequent sections, and as illustrated in Figure 4.1, this circulation system is characterized by northward flowing warm, saline water in the upper layers of the Atlantic (red curve in Fig. 4.1), a cooling and freshening of the water at higher northern latitudes of the Atlantic in the Nordic and Labrador Seas, and southward flowing colder water at depth (light blue curve). This circulation transports heat from the South Atlantic and tropical North Atlantic to the sub-polar and polar North Atlantic, where that heat is released to the atmosphere with substantial impacts on climate over large regions.

Variations in the poleward transport of heat by the oceans have the potential to make significant changes in the climate system on a variety of space and time scales.
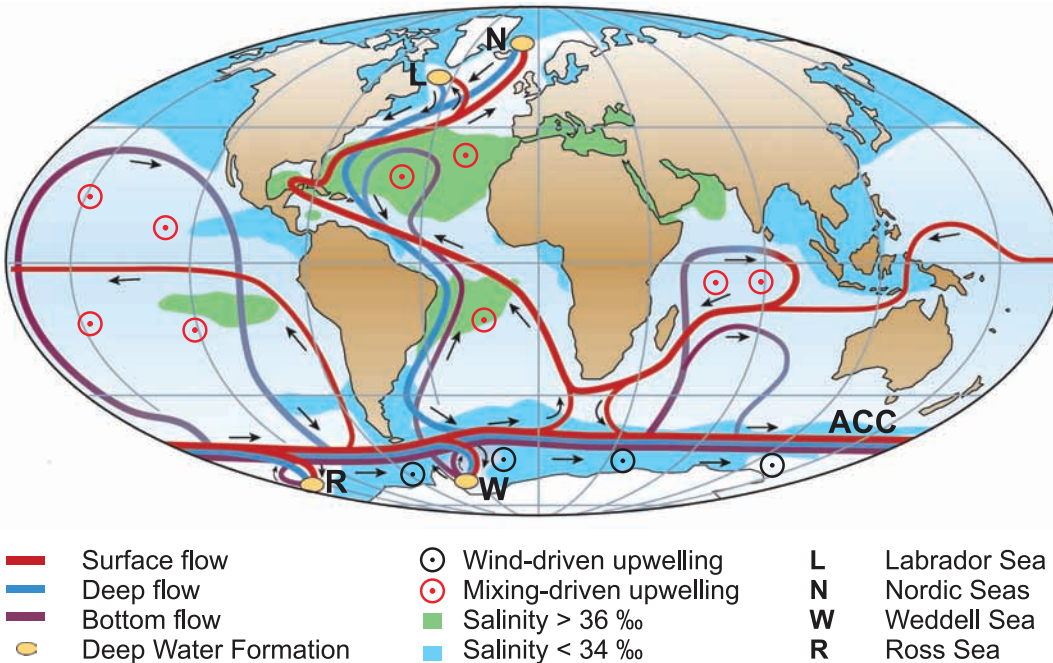

▬▬	Surface flow	⊙ Wind-driven upwelling	**L**	Labrador Sea
▬▬	Deep flow	⊙ Mixing-driven upwelling	**N**	Nordic Seas
▬▬	Bottom flow	▇ Salinity > 36 ‰	**W**	Weddell Sea
◔	Deep Water Formation	▇ Salinity < 34 ‰	**R**	Ross Sea

Figure 4.1. Schematic of the ocean circulation (from Kuhlbrodt *et al.,* 2007) associated with the global Meridional Overturning Circulation (MOC), with special focus on the Atlantic section of the flow (AMOC). The red curves in the Atlantic indicate the northward flow of water in the upper layers. The filled orange circles in the Nordic and Labrador Seas indicate regions where near-surface water cools and becomes denser, causing the water to sink to deeper layers of the Atlantic. This process is referred to as "water mass transformation," or "deep water formation." In this process heat is released to the atmosphere. The light blue curve denotes the southward flow of cold water at depth. At the southern end of the Atlantic, the AMOC connects with the Antarctic Circumpolar Current (ACC). Deep water formation sites in the high latitudes of the Southern Ocean are also indicated with filled orange circles. These contribute to the production of Antarctic Bottom Water (AABW), which flows northward near the bottom of the Atlantic (indicated by dark blue lines in the Atlantic). The circles with interior dots indicate regions where water upwells from deeper layers to the upper ocean. (See Section 2 for more discussion on where upwelling occurs as part of the global MOC.)

The Atlantic branch of this global MOC (see Fig. 4.1) consists of two primary overturning cells: (1) an "upper" cell in which warm upper ocean waters flow northward in the upper 1,000 meters (m) to supply the formation of North Atlantic Deep Water (NADW), which returns southward at depths of approximately 1,500–4,500 m and (2) a "deep" cell in which Antarctic Bottom Waters (AABW) flow northward below depths of about 4,500 m and gradually rise into the lower part of the southward-flowing NADW. Of these two cells, the upper cell is by far the stronger and is the most important to the meridional transport of heat in the Atlantic, owing to the large temperature difference (~15 °C) between the northward-flowing upper ocean waters and the southward-flowing NADW.

In assessing the "state of the AMOC," we must be clear to define what this means and how it relates to other common terminology. The terms Atlantic Meridional Overturning Circulation (AMOC) and Thermohaline Circulation (THC) are often used interchangeably but have distinctly different meanings. The AMOC is defined as the total (basin-wide) circulation in the latitude depth plane, as typically quantified by a meridional transport streamfunction. Thus, at any given latitude, the maximum value of this streamfunction, and the depth at which this occurs, specifies the total amount of water moving meridionally above this depth (and below it, in the reverse direction). The AMOC, by itself, does not include any information on what drives the circulation.

In contrast, the term "THC" implies a specific driving mechanism related to creation

and destruction of buoyancy. Rahmstorf (2002) defines this as "currents driven by fluxes of heat and freshwater across the sea surface and subsequent interior mixing of heat and salt." The total AMOC at any specific location may include contributions from the THC, as well as contributions from wind-driven overturning cells. It is difficult to cleanly separate overturning circulations into a "wind-driven" and "buoyancy-driven" contribution. Therefore, nearly all modern investigations of the overturning circulation have focused on the strictly quantifiable definition of the AMOC as given above. We will follow the same approach in this report, while recognizing that changes in the thermohaline forcing of the AMOC, and particularly those taking place in the high latitudes of the North Atlantic, are ultimately most relevant to the issue of abrupt climate change.

There is growing evidence that fluctuations in Atlantic sea surface temperatures (SSTs), hypothesized to be related to fluctuations in the AMOC, have played a prominent role in significant climate fluctuations around the globe on a variety of time scales. Evidence from the instrumental record (based on the last ~130 years) shows pronounced, multidecadal swings in SST averaged over the North Atlantic. These multidecadal fluctuations may be at least partly a consequence of fluctuations in the AMOC. Recent modeling and observational analyses have shown that these multidecadal shifts in Atlantic temperature exert a substantial influence on the climate system ranging from modulating African and Indian monsoonal rainfall to influencing tropical Atlantic atmospheric circulation conditions relevant to hurricanes. Atlantic SSTs also influence summer climate conditions over North America and Western Europe.

Evidence from paleorecords (discussed more completely in subsequent sections) suggests that there have been large, decadal-scale changes in the AMOC, particularly during glacial times. These abrupt change events have had a profound impact on climate, both locally in the Atlantic and in remote locations around the globe. Research suggests that these abrupt events were related to massive discharges of freshwater into the North Atlantic from collapsing land-based ice sheets. Temperature changes of more than

10 °C on time scales of a decade or two have been attributed to these abrupt change events.

In this chapter, we assess whether such an abrupt change in the AMOC is likely to occur in the future in response to increasing greenhouse gases. Specifically, there has been extensive discussion, both in the scientific and popular literature, about the possibility of a major weakening or even complete shutdown of the AMOC in response to global warming, along with rapid changes in land-based ice sheets (see Chapter 2) and Arctic sea ice (see Box 4.1). As will be discussed more extensively below, global warming tends to weaken the AMOC both by warming the upper ocean in the subpolar North Atlantic and through enhancing the flux of freshwater into the Arctic and North Atlantic. Both processes reduce the density of the upper ocean in the North Atlantic, thereby stabilizing the water column and weakening the AMOC. These processes could cause a weakening or shutdown of the AMOC that could significantly reduce the poleward transport of heat in the Atlantic, thereby possibly leading to regional cooling in the Atlantic and surrounding continental regions, particularly Western Europe.

In this chapter, we examine (1) our present understanding of the mechanisms controlling the AMOC, (2) our ability to monitor the state of the AMOC, (3) the impact of the AMOC on climate from observational and modeling studies, and (4) model-based studies that project the future evolution of the AMOC in response to increasing greenhouse gases and other changes in atmospheric composition. We use these results to assess the likelihood of an abrupt change in the AMOC. In addition, we note the uncertainties in our understanding of the AMOC and in our ability to monitor and predict the AMOC. These uncertainties form important caveats concerning our central conclusions.

2. WHAT ARE THE PROCESSES THAT CONTROL THE OVERTURNING CIRCULATION?

We first review our understanding of the fundamental driving processes for the AMOC. We break this discussion into two parts: the main discussion deals with the factors that are thought to be important for the equilibrium state of the AMOC, while the last part (Sec. 2.5) discusses factors of relevance for transient changes in the AMOC.

Like any other steady circulation pattern in the ocean, the flow of the Atlantic Meridional Overturning Circulation must be maintained against the dissipation of energy on the smallest length scales. We wish to determine what processes provide the energy that maintains the steady state AMOC. In general, the energy sources for the ocean are wind stress at the surface, tidal motion, heat fluxes from the atmosphere, and heat fluxes through the ocean bottom.

2.1 Sandström's Experiment

We consider the surface heat fluxes first. They are distributed asymmetrically over the globe. The ocean gains heat in the low latitudes close to the Equator and loses heat in the high latitudes toward the poles. Is this meridional gradient of the surface heat fluxes sufficient for driving a deep overturning circulation? The first one to think about this question was the Swedish researcher Sandström (1908). He conducted a series of tank experiments. His tank was narrow, but long and deep, thus putting the stress on a two-dimensional circulation pattern. He applied heat sources and cooling devices at different depths and observed whether a deep overturning circulation developed. If he applied heating and cooling both at the surface of the fluid, then he could see the water sink under the cooling device. This downward motion was compensated by a slow, broadly distributed upward motion. The resulting overturning circulation ceased

The ocean gains heat in the low latitudes close to the Equator and loses heat in the high latitudes toward the poles.

Box 4.1. Possibility for Abrupt Transitions in Sea Ice Cover

Because of certain properties of sea ice, it is quite possible that the ice cover might undergo rapid change in response to modest forcing. Sea ice has a strong inherent threshold in that its existence depends on the freezing temperature of sea water. Additionally, strong positive feedbacks associated with sea ice act to accelerate its change. The most notable of these is the positive surface albedo feedback in which changes in ice cover and surface properties modify the surface reflection of solar radiation. For example, in a warming climate, reductions in ice cover expose the dark underlying ocean, allowing more solar radiation to be absorbed. This enhances the warming and leads to further ice melt. Thus, even moderate changes in something like the ocean heat transport associated with AMOC variability could induce a large and rapid retreat of sea ice, in turn amplifying the initial warming. Indeed, a number of studies (*e.g.,* Dansgaard *et al.,* 1989; Denton *et al.,* 2005; Li *et al.,* 2005) have suggested that changes in sea-ice extent played an important role in the abrupt climate warming associated with Dansgaard-Oeschger (D-O) oscillations (see Sec. 4.5).

Abrupt, nonlinear behavior in the sea-ice cover has been simulated in simple models. For example, box model studies have shown a "switch-like" behavior in the ice cover (Gildor and Tziperman, 2001). Since the ice cover modifies ocean-atmosphere moisture exchange, this in turn affects the source of water for ice sheet growth within these models with possible implications for glacial cycles.

Other simple models, specifically diffusive climate models, also exhibit rapid sea-ice change. These models simulate that an ice cap of sufficiently small size is unstable. This "small ice cap instability" (SICI) (North, 1984) leads to an abrupt transition to year-round ice-free conditions under a gradually warming climate. Recently, Winton (2006) examined coupled climate model output and found that of two models that simulate a complete loss of Arctic ice cover in response to increased CO_2 forcing, one had SICI-like behavior in which a nonlinear response of surface albedo to the warming climate resulted in an abrupt loss of Arctic ice. The other model showed a more linear response. Perhaps more important for 21st century climate change is the possibility for a rapid transition to seasonally ice-free Arctic conditions. The summer Arctic sea-ice cover has undergone dramatic retreat since satellite records began in 1979, amounting to a loss of almost 30% of the September ice cover in 29 years. The late summer ice extent in 2007 was particularly startling and shattered the previous record minimum with an extent that was three standard deviations below the linear trend, as shown in Box 4.1 Figure 1 (from Stroeve *et al.,* 2007). Conditions over the 2007–2008 winter have promoted further loss of multiyear ice due to anomalous transport through Fram Strait, raising the possibility that rapid and sustained ice loss could result. However, at the time of this writing, it is unclear how this will ultimately affect the 2008 end-of-summer conditions, and there is little scientific consensus that another extreme minimum will occur (http://www.arcus.org/search/seaiceoutlook/report_may.php).

Climate model simulations suggest that rapid and sustained September Arctic ice loss is likely in future 21st century climate projections (Holland *et al.,* 2006). In one simulation, a transition from conditions similar to pre-2007 levels to a near-ice-free September extent occurred in a decade. Increasing ocean heat transport was implicated in this simulated rapid ice loss, which ultimately resulted from the interaction of large, intrinsic variability and anthropogenically forced change. It is notable that climate models are generally conservative in the modeled rate of Arctic ice loss as compared to observations (Stroeve *et al.,* 2007), suggesting that future ice retreat could occur even more abruptly than simulated in almost all current models.
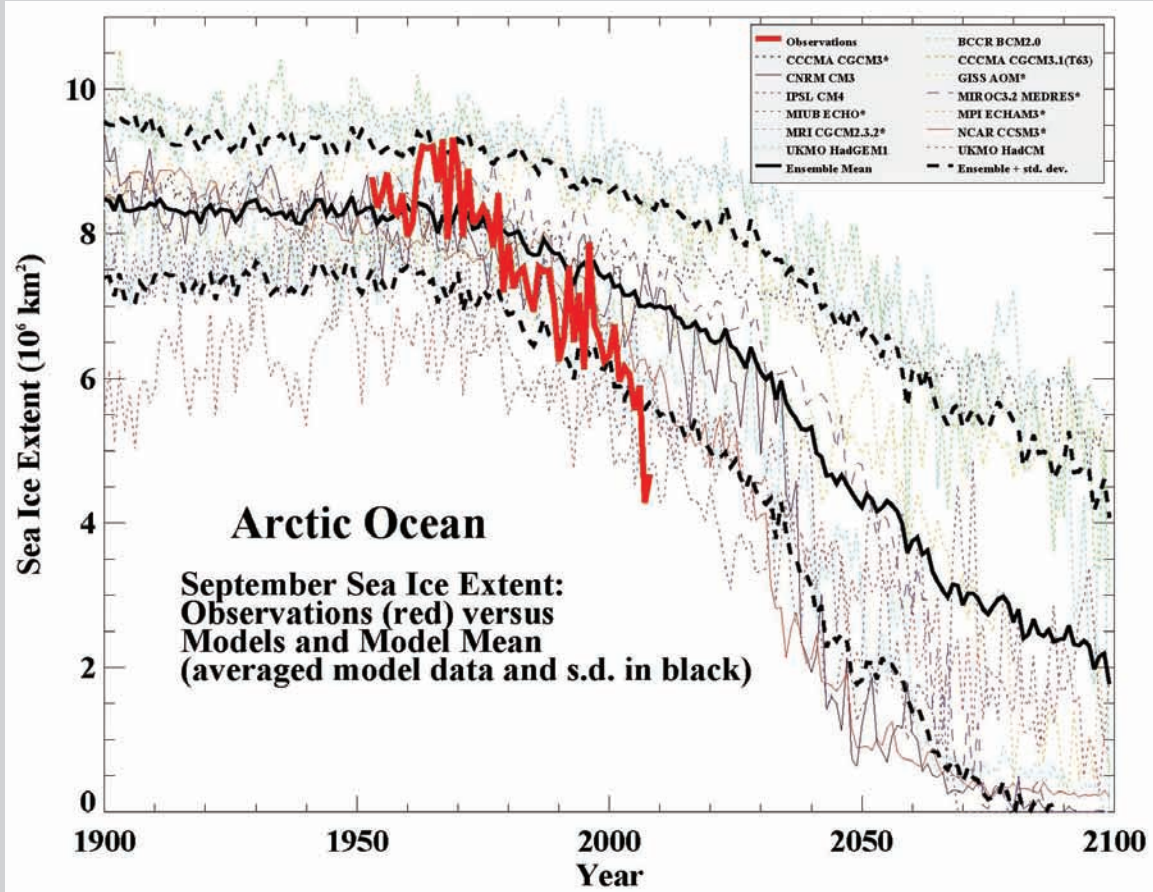
Box 4.1. Figure 1. Arctic September sea ice extent (× 10⁶ km²) from observations (thick red line) and 13 IPCC AR4 climate models, together with the multi-model ensemble mean (solid black line) and standard deviation (dotted black line). Models with more than one ensemble member are indicated with an asterisk. From Stroeve *et al.,* 2007 (updated to include 2008).

once the tank was completely filled with cold water. In addition there developed an extremely shallow overturning circulation in the topmost few centimeters, with warm water flowing toward the cooling device directly at the surface and cooler waters flowing backwards directly underneath. This pattern persisted, but a deep, top-to-bottom overturning circulation did not exist in the equilibrium state.

However, when Sandström (1908) put the heat source at depth, then such a deep overturning circulation developed and persisted. Sandström inferred that a heat source at depth is necessary to drive a deep overturning circulation in an equilibrium state. Sources and sinks of heat applied at the surface only can drive vigorous

convective overturning for a certain time, but not a steady-state circulation. The tank experiments have been debated and challenged ever since (recently reviewed by Kuhlbrodt *et al.,* 2007), but what Sandström inferred for the overturning circulation observed in the ocean remains true. Thus, if we want to understand the AMOC in a thermodynamical way, we need to determine how heat reaches the deep ocean.

One potential heat source at depth is geothermal heating through the ocean bottom. While it seems to have a stabilizing effect on the AMOC (Adcroft *et al.,* 2001), its strength of 0.05 Terawatt (TW, 1 TW = 10^{12} W) is too small to drive the circulation as a whole. Having ruled this out, the only other heat source comes from the

surface fluxes. A classical assumption is that vertical mixing in the ocean transports heat downward (Munk, 1966). This heat warms the water at depth, decreasing its density and causing it to rise. In other words, vertical advection w of temperature T and its vertical mixing, parameterized as diffusion with strength κ, are in balance:

$$w\frac{\partial T}{\partial z} = \frac{\partial}{\partial z}\kappa\frac{\partial T}{\partial z}$$

(where z denotes the vertical direction). The mixing due to molecular motion is far too small for this purpose: the respective mixing coefficient κ is on the order of $10^{-7}\,\mathrm{m^2\,s^{-1}}$. To achieve the observed upwelling of about 30 Sverdrups (Sv, where 1 Sv $= 10^6\,\mathrm{m^3\,s^{-1}}$), a vertical mixing with a global average strength of $\kappa = 10^{-4}\,\mathrm{m^2\,s^{-1}}$ is required (Munk and Wunsch, 1998; Ganachaud and Wunsch, 2000). This is presumably accomplished by turbulent mixing.

2.2 Mixing Energy Sources
In order to investigate whether there is enough energy available to drive this mixing, we turn to the schematic overview presented in Figure 4.1. We have already mentioned the heat fluxes through the surface. They are essential because the AMOC is a thermally direct circulation. The other two relevant energy sources of the ocean are winds and tides. The wind stress generates surface waves and acts on the large-scale circulation. Important for vertical mixing at depth are internal waves that are generated in the surface layer and radiate through the ocean. They finally dissipate by turbulence on the smallest length scale and the water mixes. The interaction of tidal motion with the ocean bottom also generates internal waves, especially where the topography is rough. Again, these internal waves break and dissipate, creating turbulent mixing.

Analysis of the mixing energy budget of the ocean (Munk and Wunsch, 1998; Wunsch and Ferrari, 2004) shows that the mixing energy that is available from those energy sources, about 0.4 TW, is just what is needed when one assumes that all 30 Sv of deep water that are globally formed are upwelled from depth by the advection-diffusion balance. However, the estimates of the magnitude of the terms in the mixing budget are highly uncertain. On the one hand, some studies suggest that less than these 0.4 TW are required (*e.g.,* Hughes and Griffiths, 2006). On the other hand, the mixing efficiency, a crucial parameter in the computation of this budget, might be smaller than previously thought (Arneborg, 2002), which would increase the required energy. Therefore, it cannot be determined whether the mixing energy budget is actually closed. This motivated the search for other possible driving mechanisms for the AMOC.

2.3 Wind-Driven Upwelling in the Southern Ocean
Toggweiler and Samuels (1993a, 1995, 1998) proposed a completely different driving mechanism. The surface wind forcing in the Southern Ocean leads to a northward volume transport. Due to the meridional shear of the winds, this "Ekman" transport is divergent south of 50 °S, and thus water needs to upwell from below the surface to fulfill continuity. The situation is special in the Southern Ocean in that it forms a closed circle around the Earth, with the Drake Passage between South America as the narrowest and shallowest (about 2,500 m) place (outlined dashed in Fig. 4.2). No net zonal pressure gradient can be maintained above the sill, and so no net meridional flow balanced by such a large-scale pressure gradient can exist. However, other types of flow are possible—wind-driven for instance. According to Toggweiler and Samuels (1995) this Drake Passage effect means that the waters drawn upward by the Ekman divergence must come from below the sill depth, as only from there can they be advected meridionally. Thus we have southward advection at depth, wind-driven upwelling in the Southern Ocean, and northward Ekman transport at the surface. The loop would be closed by the deep water formation in the northern North Atlantic, as that is where deep water of the density found at around 2,500 m depth is formed.

Evidence from observed tracer concentrations supports this picture of the AMOC. A number of studies (*e.g.,* Toggweiler and Samuels, 1993b; Webb and Suginohara, 2001) question that deep upwelling occurs in a broad, diffuse manner, and rather point toward substantial upwelling of deep water masses in the Southern Ocean. From model studies it is not clear to what extent
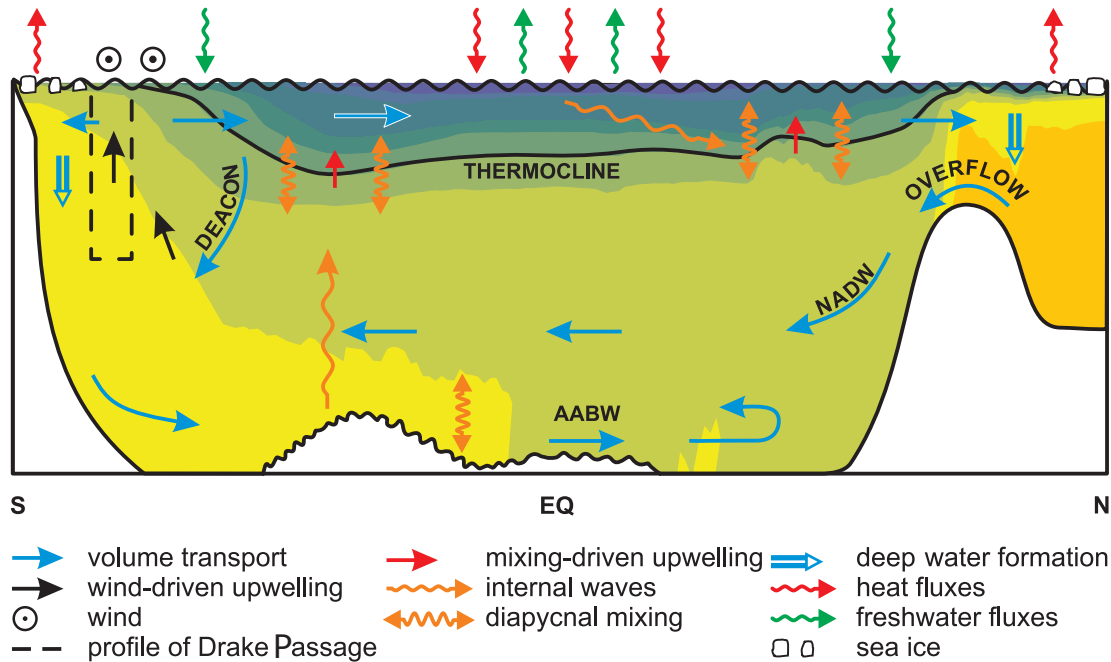
Figure 4.2. A schematic meridional section of the Atlantic Ocean representing a zonally averaged picture (from Kuhlbrodt *et al.,* 2007). The AMOC is denoted by straight blue arrows. The background color shading depicts a zonally averaged density profile from observational data. The thermocline lies between the warmer, lighter upper layers and the colder, deeper waters. Short, wavy orange arrows indicate diapycnal mixing, *i.e.,* mixing along the density gradient. This mainly vertical mixing is the consequence of the dissipation of internal waves (long orange arrows). It goes along with warming at depth that leads to upwelling (red arrows). Black arrows denote wind-driven upwelling caused by the divergence of the surface winds in the Southern Ocean together with the Drake Passage effect (explained in the text). The Deacon cell is a wind-driven regional recirculation. The surface fluxes of heat (red wavy arrows) and freshwater (green wavy arrows) are often subsumed as buoyancy fluxes. The heat loss in the northern and southern high latitudes leads to cooling and subsequent sinking, *i.e.,* formation of the deep water masses North Atlantic Deep Water (NADW) and Antarctic Bottom Water (AABW). The blue double arrows subsume the different deep water formation sites in the North Atlantic (Nordic Seas and Labrador Sea) and in the Southern Ocean (Ross Sea and Weddell Sea).

wind-driven upwelling is a driver of the AMOC. Recent studies show a weaker sensitivity of the overturning with higher model resolution, casting light on the question as to how strong the regional eddy-driven recirculation is (Hallberg and Gnanadesikan, 2006). This could compensate for the northward Ekman transport well above the depth of Drake Passage, short-circuiting the return flow.

As with the mixing energy budget, the estimates of the available energy for wind-driven upwelling are fraught with uncertainty. The work done by the surface winds on that part of the flow that is balanced by the large-scale pressure gradients can be used for wind-driven upwelling from depth. Estimates are between 1 TW (Wunsch, 1998) and 2 TW (Oort *et al.,* 1994).

2.4 Two Drivers of the Equilibrium Circulation

We define a 'driver' as a process that supplies energy to maintain a steady-state AMOC against dissipation. We find that there are two drivers that are physically quite different from each other. Mixing-driven upwelling (case 1 in Fig. 4.3) involves heat flux through the ocean across the surfaces of constant density to depth. The water there expands and then rises to the surface. By contrast, wind-driven upwelling (case 2) means that the waters are pulled to the surface along surfaces of constant density; the water changes its density at the surface when it is in contact with the atmosphere. No interior heat flux is required.
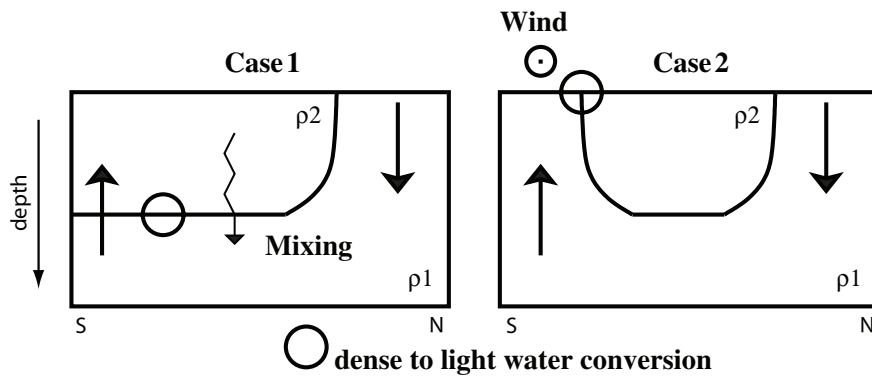
Figure 4.3. Sketch of the two driving mechanisms, mixing (case 1) and wind-driven upwelling (case 2). The sketches are schematic pictures of meridional sections of the Atlantic. Deep water is formed at the right-hand side of the boxes and goes along with heat loss. The curved solid line separates deep dense water ($\rho 1$) from lighter surface water ($\rho 2$). The solid arrows indicate volume flux; the zigzag arrow denotes downward heat flux. Figure from Kuhlbrodt *et al.* (2007).

In the real ocean, probably both driving processes play a role, as indicated by some recent studies (*e.g.,* Sloyan and Rintoul, 2001). If part of the deep water is upwelled by mixing and part by the Ekman divergence in the Southern Ocean, then the tight closure of the energy budget is not a problem anymore (Webb and Suginohara, 2001). The question about the drivers is relevant because it implies different sensitivities of the AMOC to changes in the surface forcing, and thus different ways in which climate change can affect it.

2.5 Heat and Freshwater: Relevance for Near-Term Changes

So far we have talked about the equilibrium state of the AMOC to which we applied our energy-based analysis. In models, this equilibrium is reached only after several millennia, owing to the slow time scales of diffusion. However, if we wonder about possible AMOC changes in the next decades or centuries, then model studies show that these are mainly caused by heat and freshwater fluxes at the surface (*e.g.,* Gregory *et al.,* 2005), while in principle, changes in the wind forcing may also affect the AMOC on short time scales. One can imagine that the drivers ensure that there is an overturning circulation at all, while the distribution of the heat and freshwater fluxes shapes the three-dimensional extent as well as the strength of the overturning circulation. The main influence of these surface fluxes on the AMOC is exerted on its sinking branch, *i.e.,* the formation of deep water masses in the northern North Atlantic. This deep water formation (DWF) occurs in the Nordic and Labrador Seas (see Fig. 4.1). Here, strong heat loss of the ocean to the atmosphere leads to a densification and subsequent sinking. Thus, one could see the driving processes as a pump, transporting the waters to the surface, and the DWF processes as the valve through which the waters flow downward (Samelson, 2004).

In the Labrador Sea, this heat loss occurs partly in deep convection events, in which the water is mixed vigorously and thoroughly down to 2,000 m or so. These events take place intermittently, each lasting for a few days and covering areas of 50 km to 100 km in width. In the Greenland Sea, the situation is different in that continuous mixing to intermediate depths (around 500 m) prevails. In addition, there is a sill between the Nordic Seas and the rest of the Atlantic (roughly sketched in Fig. 4.2). Any water masses from the Nordic Seas that are to join the AMOC must flow over this sill, whose depth is 600 m to 800 m. This implies that deep convection to depths of 2,000 m or 3,000 m is not essential for DWF in the Nordic Seas (Dickson and Brown, 1994). Hence the fact that it occurs only rarely is no indication for a weakening of the AMOC. By contrast, deep convection in the Labrador Sea shows strong interannual to decadal variability. This signal can be traced downstream in the deep southward current of North Atlantic Deep Water (Curry *et al.,* 1999). This suggests strongly that deep convection in the Labrador Sea can influence the strength of the AMOC.

Both a future warming and increased freshwater input (by more precipitation, more river runoff, enhanced transient export (including sea ice) from the Arctic, and melting inland ice) lead to a diminishing density of the surface waters in the North Atlantic. This hampers the densification of surface waters that is needed for DWF, and thus the overturning slows down. This mechanism can be inferred from data (see Sec. 4) and is reproduced at least qualitatively in the vast majority of climate models (Stouffer *et al.,* 2006). However, different climate models show different sensitivities toward an

imposed freshwater flux (Gregory *et al.,* 2005). Observations of the freshwater budget of the North Atlantic and the Arctic display a strong decadal variability of the freshwater content of these seas, governed by atmospheric circulation modes like the North Atlantic Oscillation (NAO) (Peterson *et al.,* 2006). These freshwater transports cause salinity variations (Curry *et al.,* 2003). The salinity anomalies affect the amount of deep water formation (Dickson *et al.,* 1996). Remarkably though, the strength of crucial parts of the AMOC, such as the sill overflow through Denmark Strait, has been almost constant over many years (Girton and Sanford, 2003), with a significant decrease reported only recently (Macrander *et al.,* 2005). It is therefore not clear to what degree salinity changes will affect the total overturning rate of the AMOC. In addition, it is hard to assess how strong future freshwater fluxes into the North Atlantic might be. This is due to uncertainties in modeling the hydrological cycle in the atmosphere (Zhang *et al.,* 2007b), in modeling the sea-ice dynamics in the Arctic, as well as in estimating the melting rate of the Greenland ice sheet (see Sec. 7).

It is important to distinguish between an AMOC weakening and an AMOC collapse. In global warming scenarios, nearly all coupled General Circulation Model's (GCMs) show a weakening in the overturning strength (Gregory *et al.,* 2005). Sometimes this goes along with a termination of deep water formation in one of the main deep water formation sites (Nordic Seas and Labrador Sea; *e.g.,* Wood *et al.,* 1999; Schaeffer *et al.,* 2002). This leads to strong regional climate changes, but the AMOC as a whole keeps going. By contrast, in some simpler coupled climate models, the AMOC collapses altogether in reaction to increasing atmospheric CO_2 (*e.g.,* Rahmstorf and Ganopolski, 1999): the overturning is reduced to a few Sverdrups. Current GCMs do not show this behavior in global warming scenarios, but a transient collapse can always be triggered in models by a large enough freshwater input and has climatic impacts on the global scale (*e.g.,* Vellinga and Wood, 2007). In some models, the collapsed state can last for centuries (Stouffer *et al.,* 2006) and might be irreversible.

Finally, it should be mentioned that the driving mechanisms of AMOC's volume flux are not
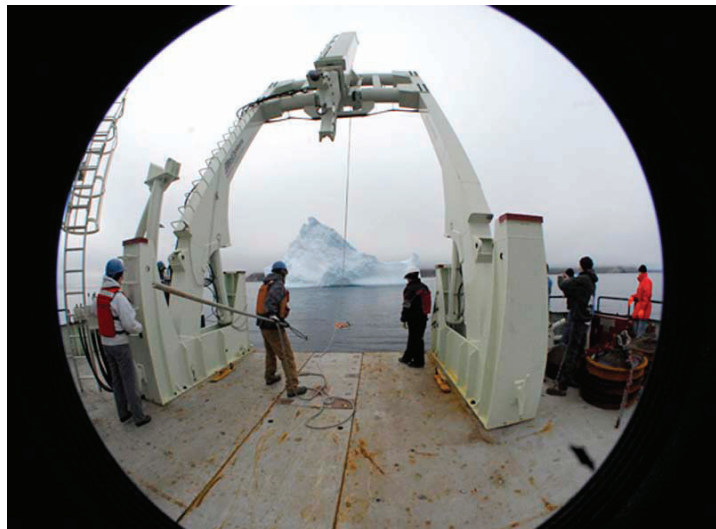
necessarily the drivers of the northward heat transport in the Atlantic (*e.g.,* Gnanadesikan *et al.,* 2005). In other words, changes of the AMOC do not necessarily have to affect the heat supply to the northern middle and high latitudes, because other current systems, eddy ocean fluxes, and atmospheric transport mechanisms can to some extent compensate for an AMOC weakening in this respect.

The result of all the mentioned uncertainties is a pronounced discrepancy in experts' opinions about the future of the AMOC. This was seen in a recent elicitation of experts' judgments on the response of the AMOC to climate change (Zickfeld *et al.,* 2007). When the twelve experts—paleoclimatologists, observationalists, and modelers—were asked about their individual probability estimates for an AMOC collapse given a 4 °C global warming by 2100, their answers lay between 0 and 60% (Zickfeld *et al.,* 2007). Enhanced research efforts in the future (see Sec. 8) are required in order to reduce these uncertainties about the future development of the AMOC.

3. WHAT IS THE PRESENT STATE OF THE AMOC?

The concept of a Meridional Overturning Circulation (MOC) involving sinking of cold waters in high-latitude regions and poleward return flow of warmer upper ocean waters can be traced to the early 1800s (Rumford, 1800; von Humboldt, 1814). Since then, the concept has evolved into the modern paradigm of a "global ocean conveyor" connecting a small

set of high-latitude sinking regions with more broadly distributed global upwelling patterns *via* a complex interbasin circulation (Stommel, 1958; Gordon, 1986). The general pattern of this circulation has been established for decades based on global hydrographic observations, and continues to be refined. However, measurement of the MOC remains a difficult challenge, and serious efforts toward quantifying the MOC, and monitoring its change, have developed only recently.

Current efforts to quantify the MOC using ocean observations rely on four main approaches:

1. Static ocean "inverse" models utilizing multiple hydrographic sections
2. Analysis of individual transoceanic hydrographic sections
3. Continuous time-series observations along a transoceanic section, and
4. Time-dependent ocean "state estimation" models

We describe, in turn, the fundamentals of these approaches and their assumptions, and the most recent results on the Atlantic MOC that have emerged from each one. In principle, the AMOC can also be estimated from ocean models driven by observed atmospheric forcing that are not constrained by ocean observations, or by coupled ocean-atmosphere models. There are many examples of such calculations in the literature, but we will restrict our review to those estimates that are constrained in one way or another by ocean observations.

3.1 Ocean Inverse Models
Ocean "inverse" models combine several (two or more) hydrographic sections bounding a specified oceanic domain to estimate the total ocean circulation through each section. These are often referred to as "box inverse" models because they close off an oceanic "box" defined by the sections and adjacent continental boundaries, thereby allowing conservation statements to be applied to the domain. The data used in these calculations consist of profiles of temperature and salinity at a number of discrete stations distributed along the sections. The models assume a geostrophic balance for the ocean circulation (apart from the wind-driven surface

Ekman layer) and derive the geostrophic velocity profile between each pair of stations, relative to an unknown reference constant, or "reference velocity." The distribution of this reference velocity along each section, and therefore the absolute circulation, is determined by specifying a number of constraints on the circulation within the box and then solving a least-squares (or other mathematical optimization) problem that best fits the constraints, within specified error tolerances. The specified constraints can be many but typically include—above all—overall mass conservation within the box, mass conservation within specified layers, independent observational estimates of mass transports through parts of the sections (*e.g.,* transports derived from current meter arrays), and conservation of property transports (*e.g.,* salt, nutrients, geochemical tracers). Increasingly, the solutions may also be constrained by estimates of surface heat and freshwater fluxes. Once a solution is obtained, the transport profile through each section can be derived, and the AMOC (for zonal basin-spanning sections) can be estimated.

The most comprehensive and up-to-date inverse analyses for the global time-mean ocean include those by Ganachaud (2003a) and Lumpkin and Speer (2007) (Fig. 4.4), based on the World Ocean Circulation Experiment (WOCE) hydrographic data collected during the 1990s. The strength of the Atlantic MOC is given as 18 ± 2.5 Sv by Lumpkin and Speer (2007) near 24 °N., where it reaches its maximum value. The corresponding estimate from Ganachaud (2003a) is 16 ± 2 Sv, in agreement within the error estimates. In both analyses the AMOC strength is nearly uniform throughout the Atlantic from 20°S. to 45°N., ranging from approximately 14 to 18 Sv. These estimates should be taken as being representative of the average strength of the AMOC over the period of the observations.

An implicit assumption in these analyses is that the ocean circulation is in a "steady state" over the time period of the observations, in the above cases over a span of some 10 years. This is likely false, as estimates of relative geostrophic transports across individual repeated sections in the North Atlantic show typical variations of ± 6 Sv (Lavin *et al.,* 1998; Ganachaud, 2003a).

Measurement of the MOC remains a difficult challenge, and serious efforts toward quantifying the MOC, and monitoring its change, have developed only recently.

This variability is accounted for in the inverse models by allowing a relatively generous error tolerance on mass conservation, particularly in upper-ocean layers, which exhibit the strongest temporal variability. While this is an acknowledged weakness of the technique, it is offset by the large number of independent sections included in these (global) analyses, which tend to iron out deviations in individual sections from the time mean. The overall error estimates for the AMOC resulting from these analyses reach about 10–15% of the AMOC magnitude in the mid-latitude North Atlantic, which at the present time can probably be considered as the best constrained available estimate of the "mean" current (1990s) state of the Atlantic AMOC. However, unless repeated over different time periods, these techniques are unable to provide information on the temporal variability of the AMOC.

3.2 Individual Transoceanic Hydrographic Sections

Historically, analysis of individual transoceanic hydrographic sections has played a prominent role in estimating the strength of the AMOC and the meridional transport of heat of the oceans (Hall and Bryden, 1982). The technique is similar to that of the box inverse techniques except that only a single overall mass constraint—the total mass transport across the section—is applied. Other constraints, such as the transports of western boundary currents known from other direct measurements, can also be used where available. The general methodology is summarized in Box 4.2. Determination of the unknown "reference velocity" in the ocean interior is usually accomplished either by assuming that it is uniform across the section or by adjusting it in such a way (subject to overall mass conservation) that it satisfies other *a*
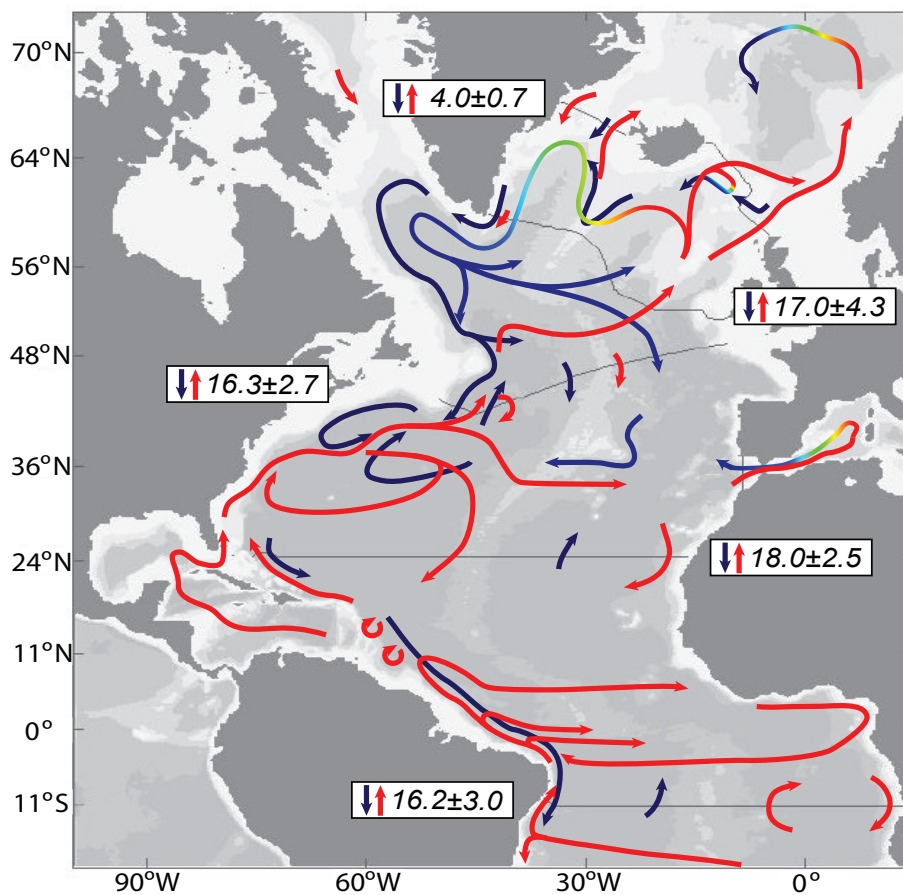

Figure 4.4. Schematic of the Atlantic MOC and major currents involved in the upper (red) and lower (blue) limbs of the AMOC, after Lumpkin and Speer (2007). The boxed numbers indicate the magnitude of the AMOC at several key locations, indicated by gray lines, along with error estimates. The red to green to blue transition on various curves denotes a cooling (red is warm, blue is cold) and sinking of the water mass along its path. Figure courtesy of R. Lumpkin, NOAA/AOML.

Box 4.2.   How Do We Measure the AMOC?

Observational estimates of the AMOC require the measurement, or inference, of all components of the meridional circulation across a basinwide section. In principle, if direct measurements of the meridional velocity profile are available at all locations across the section, the calculation of the AMOC is straightforward: the velocity is zonally integrated across the section at each depth, and the resulting vertical transport profile is then summed over the northward-moving part of the profile (which is typically the upper ~1,000 m for the Atlantic) to obtain the strength of the AMOC.

In practice, available methods for measuring the absolute velocity across the full width of a transbasin section are either prohibitively expensive or of insufficient accuracy to allow a reliable estimate of the AMOC. Thus, the meridional circulation is typically broken down into several discrete components that can either be measured directly (by current observations), indirectly (by geostrophic calculations based on hydrographic data), or inferred from wind observations (Ekman transports) or mass-balance constraints.

An illustration of this breakdown is shown in Box 4.2 Figure 1 for the specific situation of the subtropical Atlantic Ocean near 26°N., where the RAPID-MOC array is deployed and where a number of basinwide hydrographic sections have been occupied. The measured transport components include (1) direct measurement of the flow though the Straits of Florida and (2) geostrophic mid-ocean flow derived from density profiles at the eastern and western sides of the ocean, relative to an unknown constant, or "reference velocity." A third component is the ageostrophic flow in the surface layer driven by winds (the Ekman transport), which can be estimated from available wind-stress products. The only remaining unmeasured component is the depth-independent ("barotropic") mid-ocean flow, which is inferred by requiring an overall mass balance across the section. Once combined, these components define the basinwide transport profile and the AMOC strength.

The above breakdown is effective because it takes advantage of the spatially integrating nature of geostrophic computations across the interior of the ocean and limits the need for direct velocity or transport measurements to narrow regions near the coastal boundaries where swift currents may occur (in particular, in the western boundary region). The application is similar for individual hydrographic sections or moored density arrays such as used in RAPID, except that the moored arrays can provide continuous estimates of the interior flow instead of single snapshots in time. Each location where the AMOC is to be measured requires a sampling strategy tuned to the section's topography and known circulation features, but the methodology is essentially the same (Hall and Bryden, 1982; Bryden *et al.,* 1991; Cunningham *et al.,* 2007). Inverse models (see Sec. 3.1) follow a similar approach but use a formalized set of constraints with specified error tolerances (*e.g.,* overall mass balance, western boundary current transports, property fluxes) to optimally determine the reference velocity distribution across a section (Wunsch, 1996).
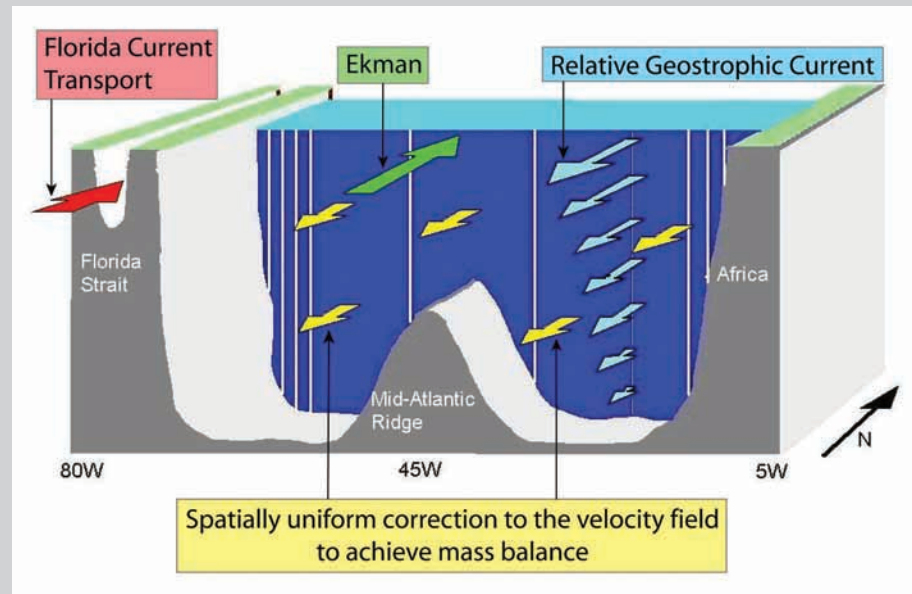
Box 4.2 Figure 1.   Circulation components required to estimate the AMOC. The figure depicts the approximate topography along 24–26°N. and the strategy employed by the RAPID monitoring array. The transport of the western boundary current is continuously monitored by a calibrated submarine cable across the Straits of Florida. Hydrographic moorings (depicted by white vertical lines) near the east and west sides of the basin monitor the (relative) geostrophic flow across the basin as well as local flow contributions adjacent to the boundaries. Ekman transport is estimated from satellite wind observations. A uniform velocity correction is included in the interior ocean to conserve mass across the section. Figure courtesy of J. Hirschi, NOC, Southampton, U.K.

priori constraints, such as the expected flow directions of specific water masses. Variability in the reference velocity is only important to the estimation of the AMOC in regions where the topography is much shallower than the mean depth of the section, which is normally confined to narrow continental margins where additional direct observations, if available, are included in the overall calculation.

The best studied location in the North Atlantic, where this methodology has been repeatedly applied to estimate the AMOC strength, is near 24°N., where a total of five transoceanic sections have been acquired between 1957 and 2004. The AMOC estimates derived from these sections range from 14.8 to 22.9 Sv, with a mean value of 18.4 ± 3.1 Sv (Bryden *et al.,* 2005). Individual sections have an estimated error of ±6 Sv, considerably larger than the error estimates from the above inverse models. Two sections that were acquired during the WOCE period (in 1992 and 1998) yield AMOC estimates of 19.4 and 16.1 Sv, respectively. Therefore, these estimates are consistent with the WOCE inverse AMOC estimates at 24°N. within their quoted uncertainty, as is the mean value of all of the sections (18.4 Sv). Bryden *et al.* (2005) note a trend in the individual section estimates, with the largest AMOC value (22.9 Sv) occurring in 1957 and the weakest in 2004 (14.8 Sv), suggesting a nearly 30% decrease in the AMOC over this period (Fig. 4.5). Taken at face value, this trend is not significant, as the total change of 8 Sv between 1957 and 2004 falls within the bounds of the error estimates. However, Bryden *et al.* (2005) argue, based upon their finding that the reduced northward transport of upper ocean waters is balanced by a reduction in only the deepest layer of southward NADW, that this change indeed likely reflects a longer term trend rather than random variability. Based upon more recent data collected within the Rapid Climate Change (RAPID) program (see below), it is now believed that the apparent trend could likely have been caused by temporal sampling aliasing.

A similar analysis of available hydrographic sections at 48°N., though less well constrained by western boundary observations than at 24°N., suggests an AMOC variation there of between 9 to 19 Sv, based on three sections

acquired between 1957 and 1992 (Koltermann *et al.,* 1999). The evidence from individual hydrographic sections therefore points to regional variations in the AMOC of order 4–5 Sv, or about ±25% of its mean value. The time scales associated with this variability cannot be established from these sections, which effectively can only be considered to be "snapshots" in time. Such estimates are, therefore, potentially vulnerable to aliasing by all time scales of AMOC variability.

3.3 Continuous Time-Series Observations
Until recently, there had never been an attempt to continuously measure the AMOC with time-series observations covering the full width and depth of an entire transoceanic section. Motivated by the uncertainty surrounding "snapshot" AMOC estimates derived from hydrographic sections, a joint U.K.-U.S. observational program, referred to as "RAPID–MOC," was mounted in 2004 to begin continuous monitoring of the AMOC at 26°N. in the Atlantic.

The overall strategy consists of the deployment of deep water hydrographic moorings (moorings with temperature and salinity recorders spanning the water column) on either side of the basin to monitor the basin-wide geostrophic shear, combined with observations from clusters of moorings on the western (Bahamas) and eastern (African) continental margins, and direct measurements of the flow though the Straits of Florida by electronic cable (see Box 4.2). Moorings are also included on the flanks of the Mid-Atlantic Ridge to resolve flows in either sub-basin. Ekman transports derived from winds (estimated from satellite measurements) are then combined with the geostrophic and direct current observations and an overall mass conservation constraint to continuously estimate the basin-wide AMOC strength and vertical structure (Cunningham *et al.,* 2007; Kanzow *et al.,* 2007).

Although only the first year of results is presently available from this program, these results provide a unique new look at AMOC variability (Fig. 4.6) and provide new insights on estimates derived from one-time hydrographic sections. The annual mean strength and standard devia-

A joint U.K.-U.S. observational program, referred to as "RAPID–MOC," was mounted in 2004 to begin continuous monitoring of the AMOC at 26°N. in the Atlantic.
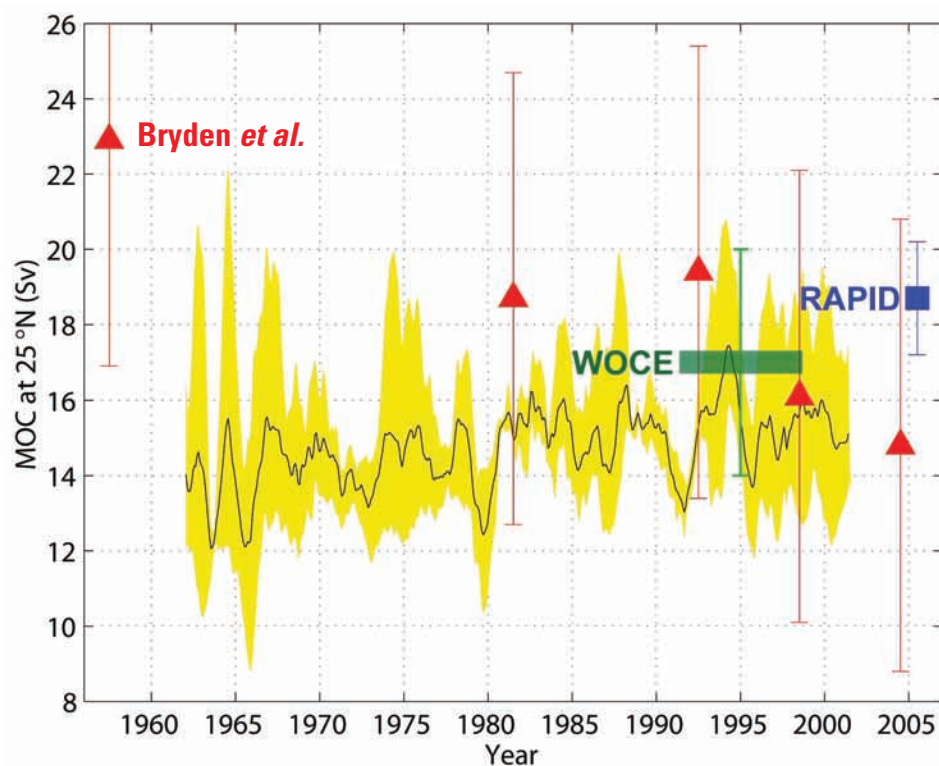
Figure 4.5.   Strength of the Atlantic MOC at 25°N. derived from an ensemble average of three state estimation models (solid curve), and the model spread (shaded), for the period 1962–2002 (courtesy of the CLIVAR Global Synthesis and Observations Panel, GSOP). The estimates from individual hydrographic sections at 24°N. (from Bryden *et al.,* 2005), from the WOCE inverse model estimates at 24°N. (Ganachaud, 2003a; Lumpkin and Speer, 2007), and from the 2004–05 RAPID–MOC array at 26°N. (Cunningham *et al.,* 2007) are also indicated, with respective uncertainties.

tion of the AMOC, from March 2004 to March 2005, was 18.7 ± 5.6 Sv, with instantaneous (daily) values varying over a range of nearly 10–30 Sv. The Florida Current, Ekman, and mid-ocean geostrophic transport were found to contribute about equally to the variability in the upper ocean limb of the AMOC. The compensating southward flow in the deep ocean (identical to the red curve in Figure 4.6 but opposite in sign), also shows substantial changes in the vertical structure of the deep flow, including several brief periods where the transport of lower NADW across the entire section (associated with source waters originating in the Norwegian-Greenland Sea dense overflows) is nearly, or totally, interrupted.

These results show that the AMOC can, and does, vary substantially on relatively short time scales and that AMOC estimates derived from one-time hydrographic sections are likely to be seriously aliased by short-term variability. Although the short-term variability

of the AMOC is large, the standard error in the 1-year RAPID estimate derived from the autocorrelation statistics of the time series is approximately 1.5 Sv (Cunningham *et al.,* 2007). Thus, this technique should be capable of resolving year-to-tear changes in the annual mean AMOC strength of the order of 1–2 Sv. The 1-year (2004–05) estimate of the AMOC strength of 18.7 ±1.5 Sv is consistent, within error estimates, with the corresponding values near 26°N. determined from the WOCE inverse analysis (16–18 ±2.5 Sv). It is also consistent with the 2004 hydrographic section estimate of 14.8 ±6 Sv, which took place during the first month of the RAPID time series (April 2004), during a period when the AMOC was weaker than its year-long average value (Fig. 4.5).

3.4 Time-Varying Ocean State Estimation

With recent advances in computing capabilities and global observations from both satellites and autonomous *in-situ* platforms,
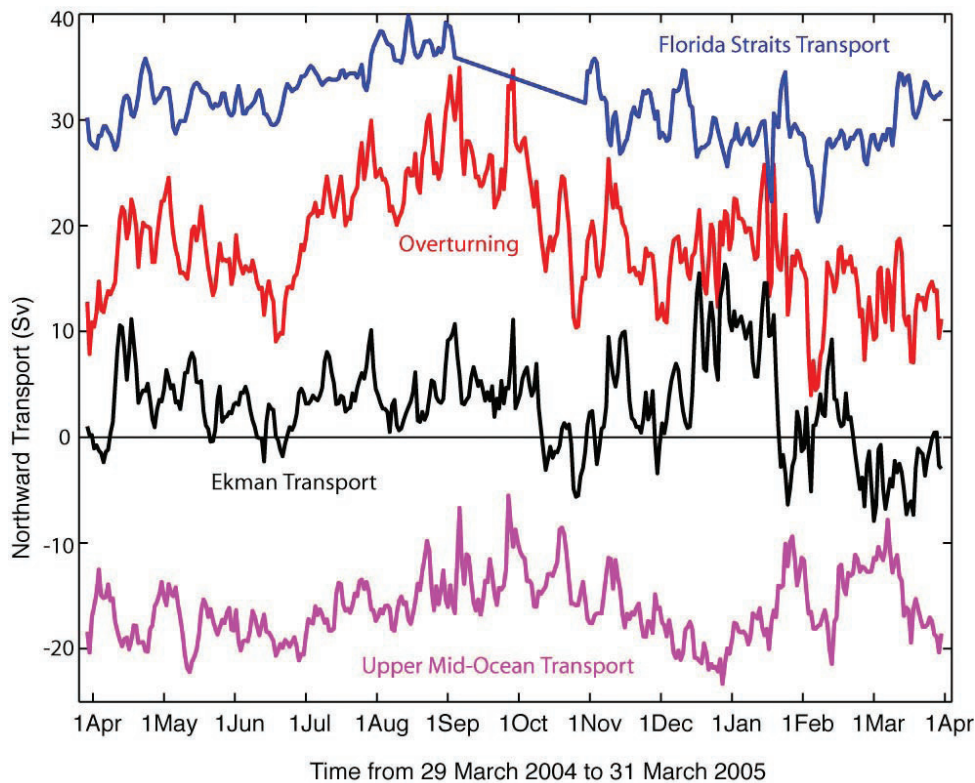
Figure 4.6. Time series of AMOC variability at 26°N. ("overturning," red curve), derived from the 2004–05 RAPID array (from Cunningham *et al.,* 2007). Individual contributions to the total upper ocean flow across the section by the Florida Current (blue), Ekman transport (black), and the mid-ocean geostrophic flow (magenta) are also shown. A 2-month gap in the Florida current transport record during September to November 2004 was caused by hurricane damage to the electromagnetic cable monitoring station on the Bahamas side of the Straits of Florida.

the field of oceanography is rapidly evolving toward operational applications of ocean state estimation analogous to that of atmospheric reanalysis activities. A large number of these activities are now underway that are beginning to provide first estimates of the time-evolving ocean "state" over the last 50+ years, during which sufficient observations are available to constrain the models.

There are two basic types of methods, (1) variational adjoint methods based on control theory and (2) sequential estimation based on stochastic estimation theory. Both methods involve numerical ocean circulation models forced by global atmospheric fields (typically derived from atmospheric reanalyses) but differ in how the models are adjusted to fit ocean data. Sequential estimation methods use specified atmospheric forcing fields to drive the models, and progressively correct the model fields in time to fit (within error tolerances) the data as they become available (*e.g.,* Carton *et al.,* 2000).

Adjoint methods use an iterative process to minimize differences between the model fields and available data over the entire duration of the model run (up to 50 years), through adjustment of the atmospheric forcing fields and model initial conditions, as well as internal model parameters (*e.g.,* Wunsch, 1996). Except for the simplest of the sequential estimation techniques, both approaches are computationally expensive, and capabilities for running global models for relatively long periods of time and at a desirable level of spatial resolution are currently limited. However, in principle these models are able to extract the maximum amount of information from available ocean observations and provide an optimum, and dynamically self-consistent, estimate of the time-varying ocean circulation. Many of these models now incorporate a full suite of global observations, including satellite altimetry and sea surface temperature observations, hydrographic stations, autonomous profiling floats, subsurface temperature profiles derived from bathythermographs, surface
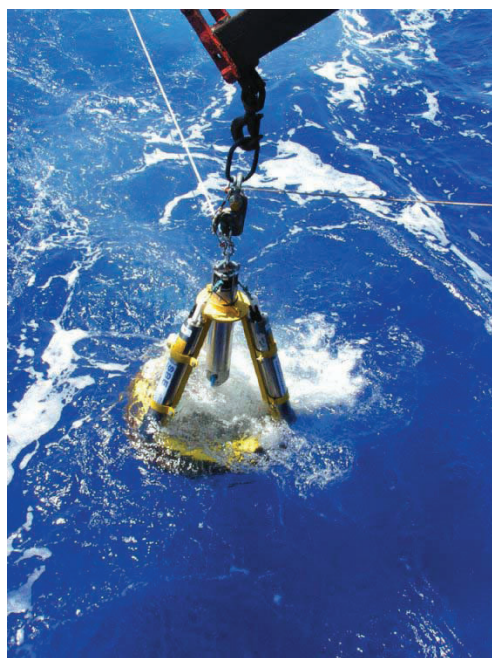
drifters, tide stations, and moored buoys.

Progress in this area is fostered by the International Climate Variability and Predictability (CLIVAR) Global Synthesis and Observations Panel (GSOP) through synthesis intercomparison and verification studies (http://www.clivar.org/organization/gsop/reference.php). A time series of the Atlantic AMOC at 25°N. derived from an ensemble average of three of these state estimation models, covering the 40-year period from 1962 to 2002, is shown in Figure 4.5. The average AMOC strength over this period is about 15 Sv, with a typical model spread of ±3 Sv. The models suggest interannual AMOC variations of 2–4 Sv with a slight increasing (though insignificant) trend over the four decades of the analysis. The mean estimate for the WOCE period (1990–2000) is 15.5 Sv, and agrees within errors with the 16–18 Sv mean AMOC estimates from the foregoing WOCE inverse analyses.

In comparing these results with the individual hydrographic section estimates, it is notable that only the 1998 (and presumably also the more recent 2004) estimates fall within the spread of the model values. However, owing to the large error bars on the individual section estimates, this disagreement cannot be considered statistically significant. The limited number of models presently available for these long analyses may also underestimate the model spread that will occur when more models are included. It should be noted that these models are formally capable of providing error bars on their own AMOC estimates, although as yet this task has generally been beyond the available computing resources. This should become a priority within climate science once feasible.

A noteworthy feature of Figure 4.5 is the apparent increase in the AMOC strength between the end of the model analysis period in 2002 and the 2004–05 RAPID estimate, an increase of some 4 Sv. The RAPID estimate lies near the top of the model spread of the preceding four decades. Whether this represents a temporary interannual increase in the AMOC that will also be captured by the synthesis models when they are extended through this period, or will represent an ultimate disagreement between the estimates, awaits determination.

3.5 Conclusions and Outlook

The main findings of this report concerning the present state of the Atlantic MOC can be summarized as follows:

The WOCE inverse model results (*e.g.,* Ganachaud, 2003b; Lumpkin and Speer, 2007) provide, at this time, our most robust estimates of the recent "mean state" of the AMOC, in the sense that they cover an analysis period of about a decade (1990–2000) and have quantifiable (and reasonably small) uncertainties. These analyses indicate an average AMOC strength in the mid-latitude North Atlantic of 16–18 Sv.

Individual hydrographic sections widely spaced in time are not a viable tool for monitoring the AMOC. However, these sections, especially when combined with geochemical observations, still have considerable value in documenting longer term property changes that may accompany changes in the AMOC, and in the estimation of meridional property fluxes including heat, freshwater, carbon, and nutrients.

Continuous estimates of the AMOC from programs such as RAPID are able to provide accurate estimates of annual AMOC strength and interannual variability, with uncertainties on the annually averaged AMOC of 1–2 Sv, comparable to uncertainties available from the WOCE inverse analyses. RAPID is planned to continue through at least 2014 and should provide a critical benchmark for ocean synthesis models.

Time-varying ocean state estimation models are still in a development phase but are now providing first estimates of AMOC variability, with ongoing intercomparison efforts between different techniques. While there is still considerable research required to further refine and validate these models, including specification

Time-varying ocean state estimation models are still in a development phase but are now providing first estimates of AMOC variability.

of uncertainties, this approach should ultimately lead to our best estimates of the large-scale ocean circulation and AMOC variability.

Our assessment of the state of the Atlantic MOC has been focused on 24°N., owing to the concentration of observational estimates there, which, in turn, is historically related to the availability of long-term, high-quality western boundary current observations at this location. The extent to which AMOC variability at this latitude, apart from that due to local wind-driven (Ekman) variability, is linked to other latitudes in the Atlantic remains an important research question. Also important are changes in the structure of the AMOC, which could have long-term consequences for climate independent of changes in overall AMOC strength. For example, changes in the relative contributions of Southern Hemisphere water masses that supply the upper ocean return flow of the cell (*i.e.,* relatively warm and salty Indian Ocean thermocline water *versus* cooler and fresher Subantarctic Mode Waters and Antarctic Intermediate Waters) could significantly impact the temperature and salinity of the North Atlantic over time and feed back on the deep water formation process.

Natural variability of the AMOC is driven by processes acting on a wide range of time scales. On intraseasonal to intrannual time scales, the dominant processes are wind-driven Ekman variability and internal changes due to Rossby or Kelvin (boundary) waves. On interannual to decadal time scales, both variability in Labrador Sea convection related to NAO forcing and wind-driven baroclinic adjustment of the ocean circulation are implicated in models (*e.g.,* Boning *et al.,* 2006). Finally, on multidecadal time scales, there is growing model evidence that large-scale observed interhemispheric SST anomalies are linked to AMOC variations (Knight *et al.,* 2005; Zhang and Delworth, 2006). Our ability to detect future changes and trends in the AMOC depends critically on our knowledge of the spectrum of AMOC variability arising from these natural causes. The identification, and future detection, of AMOC changes will ultimately rely on building a better understanding of the natural variability of the AMOC on the interannual to multidecadal time scales that make up the lower frequency end of this spectrum.

4. WHAT IS THE EVIDENCE FOR PAST CHANGES IN THE OVERTURNING CIRCULATION?

Our knowledge of the mean state and variability of the AMOC is limited by the short duration of the instrumental record. Thus, in order to gain a longer term perspective on AMOC variability and change, we turn to geologic records from past climates that can yield important insights on past changes in the AMOC and how they relate to climate changes. In particular, we focus on records from the last glacial period, for which there is evidence of changes in the AMOC that can be linked to a rich spectrum of climate variability and change. Improving our ability to characterize and understand past AMOC changes will increase confidence in our ability to predict any future changes in the AMOC, as well as the global impact of these changes on the Earth's natural systems.

The last glacial period was characterized by large, widespread and often abrupt climate changes at millennial time scales, many of which have been attributed to changes in the AMOC and its attendant feedbacks (Broecker *et al.,* 1985; Clark *et al.,* 2002a, 2007; Alley, 2007). In the following, we first summarize various types of evidence (commonly referred to as proxy records, in that they provide an indirect measure of the physical property of interest) used to infer changes in the AMOC. We then discuss the current understanding of changes in the AMOC during the following four time windows (Fig. 4.7):

> In order to gain a longer term perspective on AMOC variability and change, we turn to geologic records from past climates that can yield important insights on past changes in the AMOC and how they relate to climate changes.
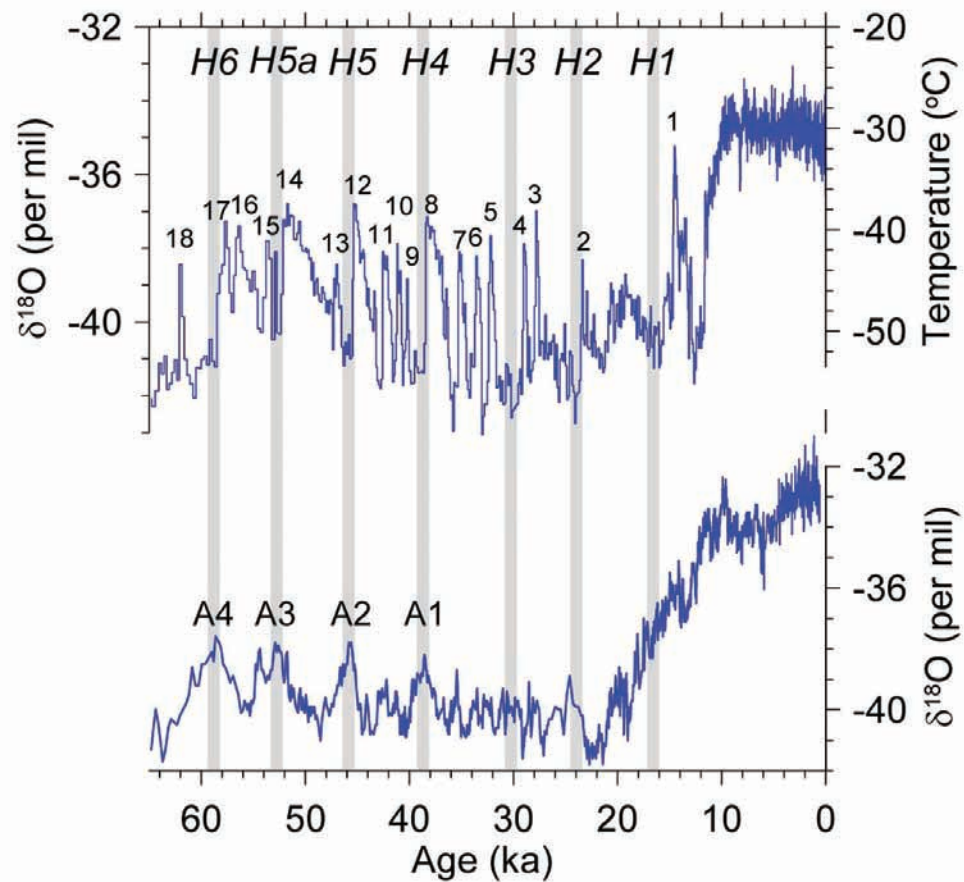
Figure 4.7. Records showing characteristic climate changes for the interval from 65,000 years ago to the present. (Top) The Greenland Ice Sheet Project (GISP2) $\delta^{18}O$ record (Grootes *et al.,* 1993; Stuiver and Grootes, 2000), which is a proxy for air temperature, with more positive values corresponding to warmer temperatures (Cuffey and Clow, 1997). Numbers 1–18 correspond to conventional numbering of warm peaks of Dansgaard-Oeschger oscillations. (Bottom) The Byrd $\delta^{18}O$ record (Johnsen *et al.,* 1972; Hammer *et al.,* 1994), with the time scale synchronized to the GISP2 time scale by methane correlation (Blunier and Brook, 2001). Antarctic warm events identified as A1, *etc.* Vertical gray bars correspond to times of Heinrich events, with each Heinrich event labeled by conventional numbering (H6, H5, *etc.*).

1. The Last Glacial Maximum (19,000–23,000 years ago), when ice sheets covered large parts of North America and Eurasia, and the concentration of atmospheric CO_2 was approximately 30% lower than during pre-industrial times. Although the Last Glacial Maximum (LGM) was characterized by relatively low climate variability at millennial time scales, it had a different AMOC than the modern AMOC, which provides a good target for the coupled climate models that are used to predict future changes.

2. The last deglaciation (11,500–19,000 years ago), which was a time of natural global warming associated with large changes in insolation, rising atmo- spheric CO_2, and melting ice sheets, but included several abrupt climate changes which likely involved changes in the AMOC.

3. Marine Isotope Stage (MIS) 3 (30,000–65,000 years ago), which was a time of pronounced millennial-scale climate variability characterized by abrupt transitions that occurred over large parts of the globe in spite of relatively small changes in insolation, atmospheric CO_2 concentration, and ice-sheet size. Just how these signals originated and were transmitted and modified around the globe, and the extent to which they are associated with changes in the AMOC, remains controversial.

4. The Holocene (0–11,500 years ago), which was a time of relative climate stability (compared to glacial climates) in spite of large changes in insolation. This period of time is characterized by atmospheric CO_2 levels similar to pre-industrial times. Although AMOC changes during the Holocene were smaller than during glacial times, our knowledge of them extends the record of natural variability under near modern boundary conditions beyond the instrumental record.

4.1 Proxy Records Used to Infer Past Changes in the AMOC

4.1.1 Water Mass Tracers

The most widely used proxy of millennial-scale changes in the AMOC is $\delta^{13}C$ of dissolved inorganic carbon, as recorded in the shells of bottom-dwelling (benthic) foraminifera, which differentiates the location, depth, and volume of nutrient-depleted North Atlantic Deep Water (NADW) relative to underlying nutrient-enriched Antarctic Bottom Water (AABW) (Boyle and Keigwin, 1982; Curry and Lohmann, 1982; Duplessy *et al.,* 1988). Millennial-scale water mass variability is also seen in the distribution of other elements linked to nutrients such as Cd and Zn in foraminifera shells (Boyle and Keigwin, 1982; Marchitto *et al.,* 1998). The radiocarbon content of deep waters (high in NADW that has recently exchanged carbon with the radiocarbon-rich atmosphere, and low in the older AABW) is recorded both in foraminifera and deep-sea corals (Keigwin and Schlegel, 2002; Robinson *et al.,* 2005) and has also been used as a water mass tracer. The deep water masses also carry a distinct Nd isotope signature, which can serve as a tracer that is independent of carbon and nutrient cycles (Rutberg *et al.,* 2000; Piotrowski *et al.,* 2005).

4.1.2 Dynamic Tracers

While the water mass tracers provide information on water mass geometry, they cannot be used alone to infer the rates of flow. Variations in the grain size of deep-sea sediments can provide information on the vigor of flow at the sediment-water interface, with stronger flows capable of transporting larger particle sizes (McCave and Hall, 2006). The magnetic properties of sediments related to particle size have also been used to infer information about the vigor of near-bottom flows (Kissel *et al.,* 1999).

The contrasting residence times of the particle-reactive decay products of dissolved uranium (Pa and Th) provide an integrated measure of the residence time of water in the overlying water column. Today, the relatively vigorous renewal of waters in the deep Atlantic results in low ratios of Pa/Th in the underlying sediments, but this ratio should increase if NADW production slows (Bacon and Anderson, 1982; Yu *et al.,* 1996). While radiocarbon has been used most successfully as a tracer of water masses in the deep Atlantic, the *in situ* decay of radiocarbon within the Atlantic could potentially be used to infer flow rates, given a sufficiently large number of precise measurements (Adkins and Boyle, 1997; Wunsch, 2003).

Finally, as for the modern ocean, we can use the fact that the large-scale oceanic flows are largely in geostrophic balance and infer flows from the distribution of density in the ocean. For paleoclimate reconstructions, the distribution of seawater density can be estimated from oxygen isotope ratios in foraminifera (Lynch-Stieglitz *et al.,* 1999) as well as other proxies for temperature and salinity (Adkins *et al.,* 2002; Elderfield *et al.,* 2006).

Most of the proxies for water mass properties and flow described above are imperfect recorders of the quantity of interest. They can also be affected to varying degrees by biological, physical, and chemical processes that are not necessarily related to deep water properties and flows. These proxies are most useful for identifying relatively large changes, and the

confidence in our inferences based on them increases when there is consistency between more than one independent line of evidence.

4.3 Evidence for State of the AMOC During the Last Glacial Maximum

Although the interval corresponding to the LGM (19,000 to 23,000 years ago) does not correspond to an abrupt climate change, a large body of evidence points to a significantly different AMOC at that time (Lynch-Stieglitz *et al.,* 2007), providing an important target for coupled climate model simulations that are used to predict future changes. Among these indicators of a different AMOC, the geographic distribution of different species of surface-dwelling (planktonic) organisms can be used to suggest latitudinal shifts in sites of deep water formation. Accordingly, while warm currents extend far into the North Atlantic today, compensating the export of deep waters from the polar seas, during the LGM, planktonic species indicate that the North Atlantic was marked by a strong east-west trending polar front separating the warm subtropical waters from the cold waters which dominated the North Atlantic during glacial times, suggesting a southward displacement of deep water formation (CLIMAP, 1981; Ruddiman and McIntyre, 1981; Paul and Schafer-Neth, 2003; Kucera *et al.,* 2005).

The chemical and isotopic compositions of benthic organisms suggest that low-nutrient NADW dominates the modern deep North Atlantic (Fig. 4.8). During the LGM, however, these proxies indicate that the deep water masses below 2 kilometers (km) depth appear to be older (Keigwin, 2004) and more nutrient rich (Duplessy *et al.,* 1988; Sarnthein *et al.,* 1994; Bickert and Mackensen, 2004; Curry and Oppo, 2005; Marchitto and Broecker, 2006) than the waters above 2 km, suggesting a northward expansion of AABW and corresponding shoaling of NADW to form Glacial North Atlantic Intermediate Water (GNAIW) (Fig. 4.8). Finally, pore-water chloride data from deep-sea sediments in the Southern Ocean indicate that the north-south salinity gradient in the deep Atlantic was reversed relative to today, with the deep Southern Ocean being much saltier than the North Atlantic (Adkins *et al.,* 2002).

The accumulation of the decay products of uranium in ocean sediments (Pa/Th ratio) is consistent with an overall residence time of deep waters in the Atlantic that was slightly longer than today (Yu *et al.,* 1996; Marchal *et al.,* 2000; McManus *et al.,* 2004). Reconstructions of seawater density based on the isotopic composition of benthic shells suggest a reduced density contrast across the South Atlantic basin, implying a weakened AMOC in the upper 2 km of the South Atlantic (Lynch-Stieglitz *et al.,* 2006). Inverse modeling (Winguth *et al.,* 1999) of the carbon isotope data is also consistent with a slightly weaker AMOC during the LGM.

4.4 Evidence for Changes in the AMOC During the Last Deglaciation

Multiple proxies indicate that the AMOC underwent several large and abrupt changes during the last deglaciation (11,500 to 19,000 years ago). Proxies of temperature and precipitation suggest corresponding changes in climate (Fig. 4.7) that can be attributed to these changes in the AMOC and its attendant feedbacks (Broecker *et al.,* 1985; Clark *et al.,* 2002a; Alley, 2007). Many of the AMOC proxy records from marine sediments show that the changes in deep water properties and flow were quite abrupt, but due to slow sedimentation rates and mixing of the sediments at the sea floor, these records can only provide an upper bound on the transition time between one circulation state and another. Radiocarbon data from fossil deep-sea corals, however, show that deep water properties can change substantially in a matter of decades (Adkins *et al.,* 1998). Several possible freshwater forcing mechanisms have been identified that may explain this variability, although there are still large uncertainties in understanding the relation between these mechanisms and changes in the AMOC (Box 4.3).

Early in the deglaciation, starting at ~19,000 years ago, water mass tracers (^{14}C and $\delta^{13}C$) suggest that low-nutrient, radiocarbon-enriched GNAIW began to contract and shoal from its LGM distribution so that by ~17.5 ka, a significant fraction of the North Atlantic basin was filled with high-nutrient, radiocarbon-depleted AABW (Fig. 4.9) (Sarnthein *et al.,* 1994; Zahn *et al.,* 1997; Curry *et al.,* 1999; Willamowski and Zahn, 2000; Rickaby and Elderfield, 2005; Robinson *et al.,* 2005). Dynamic tracers of the

Although the interval corresponding to the LGM (19,000 to 23,000 years ago) does not correspond to an abrupt climate change, a large body of evidence points to a significantly different AMOC at that time.
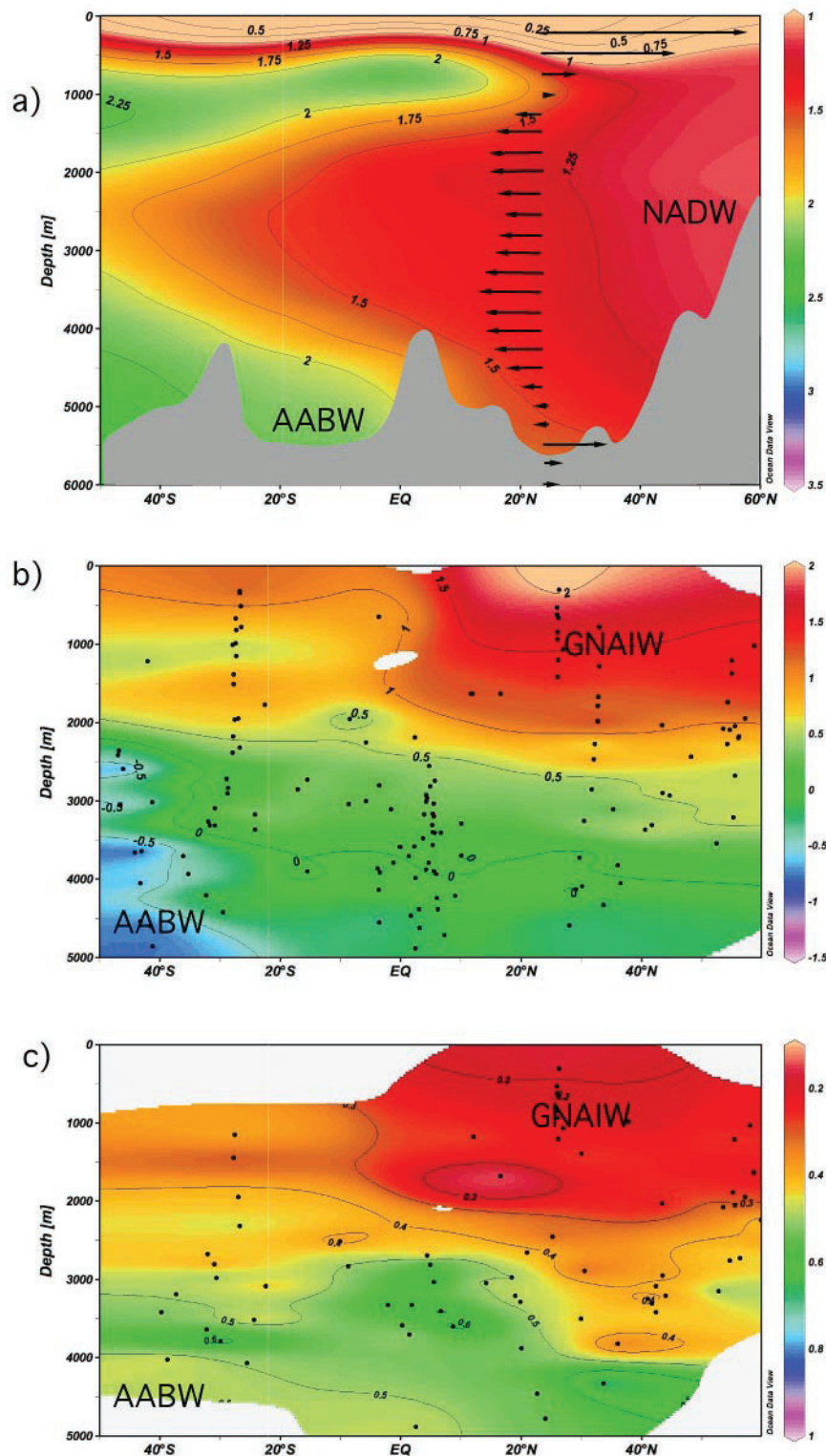
Figure 4.8. (a) The modern distribution of dissolved phosphate (PO$_4$, mmol liter^{-1})—a biological nutrient—in the western Atlantic (Conkright et al., 2002). Also indicated is the southward flow of North Atlantic Deep Water (NADW), which is compensated by the northward flow of warmer waters above 1 km, and the Antarctic Bottom Water (AABW) below. (b) The distribution of the carbon isotopic composition (^{13}C/^{12}C, expressed as δ^{13}C, Vienna Pee Dee belemnite standard) of the shells of benthic foraminifera in the western and central Atlantic during the Last Glacial Maximum (LGM) (Bickert and Mackensen, 2004; Curry and Oppo, 2005). Data (dots) from different longitudes are collapsed in the same meridional plane. GNAIW, Glacial North Atlantic Intermediate Water. (c) Estimates of the Cd (nmol kg^{-1}) concentration for LGM from the ratio of Cd/Ca in the shells of benthic foraminifera, from Marchitto and Broecker (2006). Today, the isotopic composition of dissolved inorganic carbon and the concentration of dissolved Cd in seawater both show "nutrient"-type distributions similar to that of PO$_4$.
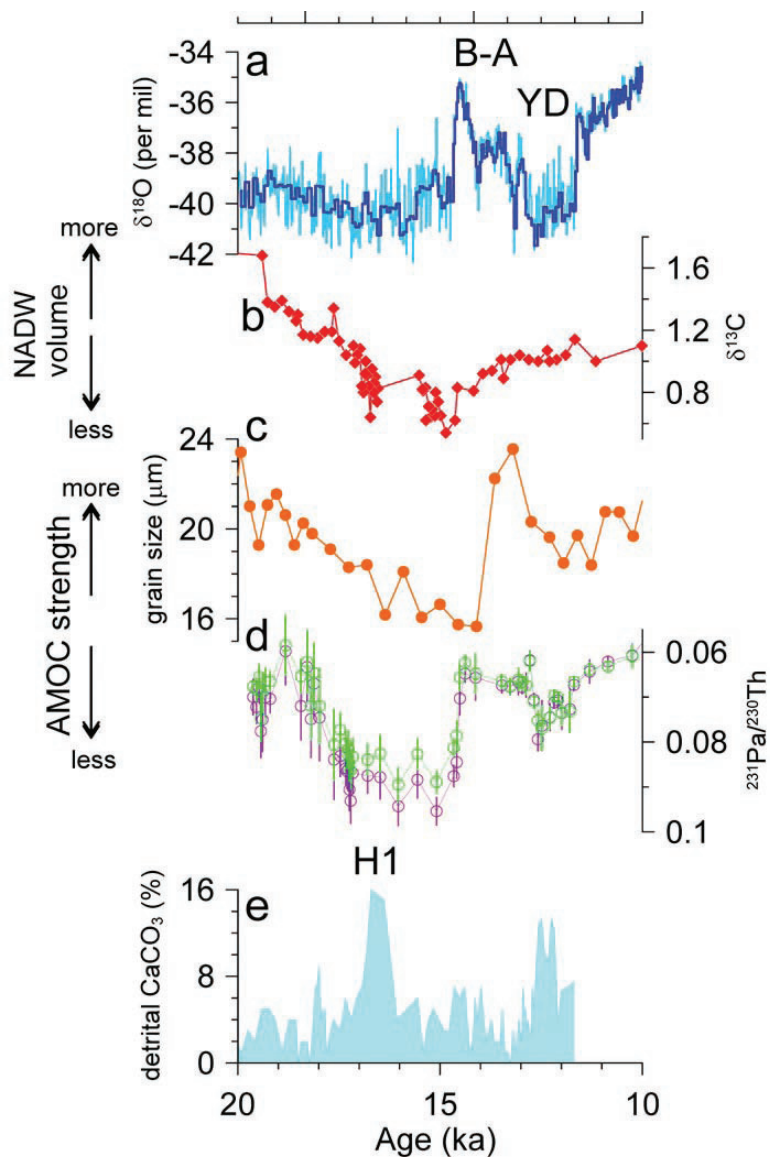
ratio at which they are produced in the water column, requiring a slowdown or shutdown of deep water renewal in the deep Atlantic (Siddall *et al.,* 2007), thus explaining the extreme contraction of GNAIW inferred from the water mass tracers. At the same time, radiocarbon data from the Atlantic basin not only support a reduced flux of GNAIW but also indicate a vigorous circulation of AABW in the North Atlantic basin (Robinson *et al.,* 2005).

The cause of this extreme slowdown of the AMOC is often attributed to Heinrich event 1, which represented a massive release of icebergs from the Laurentide Ice Sheet into the North Atlantic Ocean (Box 4.3) (Broecker, 1994; McManus *et al.,* 2004; Timmermann *et al.,* 2005b). The best estimate for the age of Heinrich event 1 (~17.5 ka), however, indicates the decrease in the AMOC began ~1,500 years earlier, with the event only coinciding with the final near-cessation of the AMOC ~17.5 ka (Fig. 4.9) (Bond *et al.,* 1993; Bond and Lotti, 1995; Hemming, 2004). These relations thus suggest that some other mechanism was responsible for the decline and eventual near-collapse of the AMOC prior to the event (Box 4.3).

This interval of a collapsed AMOC continued until ~14.6 ka, when dynamic tracers indicate a rapid resumption of the AMOC to near-interglacial rates (Fig. 4.9). This rapid change in the AMOC was accompanied by an abrupt warming throughout much of the Northern Hemisphere associated with the onset of the Bølling-Allerød warm interval (Clark *et al.,* 2002b). The renewed overturning filled the North Atlantic basin with NADW, as shown by Cd/Ca ratios (Boyle and Keigwin, 1987) and Nd isotopes (Piotrowski *et al.,* 2004) from the North and South Atlantic, respectively. Moreover, the distribution of radiocarbon in the North Atlantic was similar to the modern ocean, with the entire water column filled by radiocarbon-enriched water (Robinson *et al.,* 2005).

An abrupt reduction in the AMOC occurred again at ~12.9 ka, corresponding to the start of the ~1200-year Younger Dryas cold interval. During this time period, many of the paleoceanographic proxies suggest a return to a circulation state similar to the LGM. Unlike

Figure 4.9. Proxy records of changes in climate and the AMOC during the last deglaciation. Ka, thousand years. (a) The GISP2 $\delta^{18}O$ record (Grootes *et al.,* 1993; Stuiver and Grootes, 2000). B-A is the Bølling-Allerød warm interval, YD is the Younger Dryas cold interval, and H1 is Heinrich event 1. (b) The $\delta^{13}C$ record from core SO75-26KL in the eastern North Atlantic (Zahn *et al.,* 1997). (c) Record of changes in grain size ("sortable silt") from core BOFS 10k in the eastern North Atlantic (Manighetti and McCave, 1995). (d) The record of $^{231}Pa/^{230}Th$ in marine sediments from the Bermuda Rise, western North Atlantic (McManus *et al.,* 2004). Purple symbols are values based on total ^{238}U activity, green symbols are based on total ^{232}Th activity. (e) Record of changes in detrital carbonate from core VM23-81 from the North Atlantic (Bond *et al.,* 1997).

AMOC (grain size and Pa/Th ratios of deep-sea sediments) similarly show a shift starting at ~19 ka toward values that indicate a reduction in the rate of the AMOC (Fig. 4.9) (Manighetti and McCave, 1995; McManus *et al.,* 2004). By ~17.5 ka, the Pa/Th ratios almost reach the

Box 4.3.   Past Mechanisms for Freshwater Forcing of the AMOC

Ice sheets represent the largest readily exchangeable reservoir of freshwater on Earth. Given the proximity of modern and former ice sheets to critical sites of intermediate and deep water formation (Fig. 4.1), variations in their freshwater fluxes thus have the potential to induce changes in the AMOC. In this regard, the paleorecord has suggested four specific mechanisms by which ice sheets may rapidly discharge freshwater to the surrounding oceans and cause abrupt changes in the AMOC: (1) Heinrich events, (2) meltwater pulses, (3) routing events, and (4) floods.

1.   Heinrich events are generally thought to represent an ice-sheet instability resulting in abrupt release of icebergs that triggers a large reduction in the AMOC. Paleoclimate records, however, indicate that Heinrich events occur after the AMOC has slowed down or largely collapsed. An alternative explanation is that Heinrich events are triggered by an ice-shelf collapse induced by subsurface oceanic warming that develops when the AMOC collapses, with the resulting flux of icebergs acting to sustain the reduced AMOC.

2.   The ~20-m sea-level rise ~14,500 years ago, commonly referred to as meltwater pulse (MWP) 1A, indicates an extraordinary episode of ice-sheet collapse, with an associated freshwater flux to the ocean of ~0.5 Sv over several hundred years (see Chapter 2). Nevertheless, the timing, source, and the effect on climate of MWP-1A remain unclear. In one scenario, the event was triggered by an abrupt warming (start of the Bølling warm interval) in the North Atlantic region, causing widespread melting of Northern Hemisphere ice sheets. Although this event represents the largest freshwater forcing yet identified from paleo-sea-level records, there was little response by the AMOC, leading to the conclusion that the meltwater entered the ocean as a sediment-laden, very dense bottom flow, thus reducing its impact on the AMOC. In another scenario, MWP-1A largely originated from the Antarctic Ice Sheet, possibly in response to the prolonged interval of warming in the Southern Hemisphere that preceded the event. In this case, climate model simulations indicate that the freshwater perturbation in the Southern Ocean may have triggered the resumption of the AMOC that caused the Bølling warm interval.

3.   The most well-known hypothesis for a routing event involves retreat of the Laurentide Ice Sheet (LIS) that redirected continental runoff from the Mississippi to the St. Lawrence River, triggering the Younger Dryas cold interval. There is clear paleoceanographic evidence for routing of freshwater away from the Mississippi River at the start of the Younger Dryas, and recent paleoceanographic evidence now clearly shows a large salinity decrease in the St. Lawrence estuary at the start of the Younger Dryas associated with an increased freshwater flux derived from western Canada.

4.   The most well-known flood is the final sudden drainage of glacial Lake Agassiz that is generally considered to be the cause of an abrupt climate change ~8400 years ago. For this event, the freshwater forcing was likely large but short; the best current estimate suggests a freshwater flux of 4–9 Sv over 0.5 year. This event was unique to the last stages of the LIS, however, and similar such events should only be expected in association with similar such ice-sheet configurations. Other floods have been inferred at other times, but they would have been much smaller (~0.3 Sv in 1 year), and model simulations suggest they would have had a negligible impact on the AMOC.

the near-collapse earlier in the deglaciation at ~17.5 ka, for example, Pa/Th ratios suggest only a partial reduction in the AMOC during the Younger Dryas (Fig. 4.9). Sediment grain size (Manighetti and McCave, 1995) also shows evidence for reduced NADW input into the North Atlantic during the Younger Dryas event (Fig. 4.9). Radiocarbon concentration in the atmosphere rises at the start of the Younger Dryas, which is thought to reflect decreased ocean uptake due to a slowdown of the AMOC (Hughen *et al.,* 2000). Radiocarbon-depleted AABW replaced radiocarbon-enriched NADW below ~2500 m, suggesting a shoaling of NADW coincident with a reduction of the AMOC (Keigwin, 2004). The δ^{13}C values also suggest a return to the LGM water mass configuration (Sarnthein *et al.,* 1994; Keigwin, 2004), as do other nutrient tracers (Boyle and Keigwin, 1987) and the Nd isotope water mass tracer (Piotrowski *et al.,* 2005).

The cause of the reduced AMOC during the Younger Dryas has commonly been attributed to the routing of North American runoff with a resulting increase in freshwater flux draining eastward through the St. Lawrence River (Johnson and McClure, 1976; Rooth, 1982; Broecker *et al.,* 1989), which is supported by recent paleoceanographic evidence (Flower *et al.,* 2004; Carlson *et al.,* 2007) (Box 4.3).

4.5 Evidence for Changes in the AMOC During Stage 3

Marine isotope stage 3 (30,000–65,000 years ago) was a period of intermediate ice volume that occurred prior to the LGM. This period of time is characterized by the Dansgaard-Oeschger (D-O) oscillations, which were first identified from Greenland ice-core records (Johnsen *et al.,* 1992; Grootes *et al.,* 1993) (Fig. 4.7). These oscillations are similar to the abrupt climate changes during the last deglaciation and are characterized by alternating warm (interstadial) and cold (stadial) states lasting for millennia, with abrupt transitions between states of up to 16 °C occurring over decades or less (Cuffey and Clow, 1997; Huber *et al.,* 2006). Bond *et al.* (1993) recognized that several successive D-O oscillations of decreasing amplitude represented a longer term (~7,000-yr) climate oscillation which culminates in a massive release of icebergs from the Laurentide Ice Sheet, known as a Heinrich event (Fig. 4.7) (Box 4.3). The D-O signal seems largely confined to the Northern Hemisphere, while the Southern Hemisphere often exhibits less abrupt, smaller amplitude millennial climate changes (Clark *et al.,* 2007), best represented by A-events seen in Antarctic ice core records (Fig. 4.7). Synchronization of Greenland and Antarctic ice core records (Bender *et al.,* 1994, 1999; Sowers and Bender, 1995; Blunier *et al.,* 1998; Blunier and Brook, 2001; EPICA Community Members, 2006) suggests an out-of-phase "seesaw" relationship between temperatures of the Northern and Southern Hemispheres, and that the thermal contrast between hemispheres is greatest at the time of Heinrich events (Fig. 4.7).

By comparison to the deglaciation, there are fewer proxy records constraining millennial-scale changes in the AMOC during stage 3. Most inferences of these changes are based on $\delta^{13}C$ as a proxy for water-mass nutrient content. A depth transect of well-correlated $\delta^{13}C$ records is required in order to capture temporal changes in the vertical distribution of any given water mass, since the $\delta^{13}C$ values at any given depth may not change significantly if the core site remains within the same water mass.

Figure 4.10 illustrates one such time-depth transect of $\delta^{13}C$ records from the eastern North Atlantic that represent changes in the depth and volume (but not rate) of the AMOC during an interval (35–48 ka) of pronounced millennial-scale climate variability (Fig. 4.7). We emphasize this interval only because it encompasses a highly resolved and well-dated array of $\delta^{13}C$ records. The distinguishing feature of these records is a minimum in $\delta^{13}C$ at the same time as Heinrich events 4 and 5, indicating the near-complete replacement of nutrient-poor, high $\delta^{13}C$ NADW with nutrient-rich, low $\delta^{13}C$ AABW in this part of the Atlantic basin. The inference of a much reduced rate of the AMOC from these data is supported by the proxy records during the last deglaciation (Fig. 4.9), which indicate a similar distribution of $\delta^{13}C$ at a time when Pa/Th ratios suggest the AMOC had nearly collapsed by the time of Heinrich event 1 (see above). Insofar as we understand the interhemispheric seesaw relationship established by ice core records (Fig. 4.7) to reflect changes in the AMOC and corresponding ocean heat transport (Broecker, 1998; Stocker and Johnsen, 2003), the fact that Heinrich events during stage 3 only occur at times of maximum thermal contrast between hemispheres (cold north, warm south) further indicates that some other mechanism was responsible for causing the large reduction in the AMOC by the time a Heinrich event occurred.

While many of the Heinrich stadials show up clearly in these and other $\delta^{13}C$ records, there is often no clear distinction between D-O interstadials and non-Heinrich D-O stadials (Fig. 4.10) (Boyle, 2000; Shackleton *et al.,* 2000; Elliot *et al.,* 2002). While some $\delta^{13}C$ and Nd records do show millennial-scale variability not associated with the Heinrich events (Charles *et al.,* 1996; Curry *et al.,* 1999; Hagen and Keigwin, 2002; Piotrowski *et al.,* 2005), there are many challenges that have impeded the ability to firmly establish the presence or absence of coherent
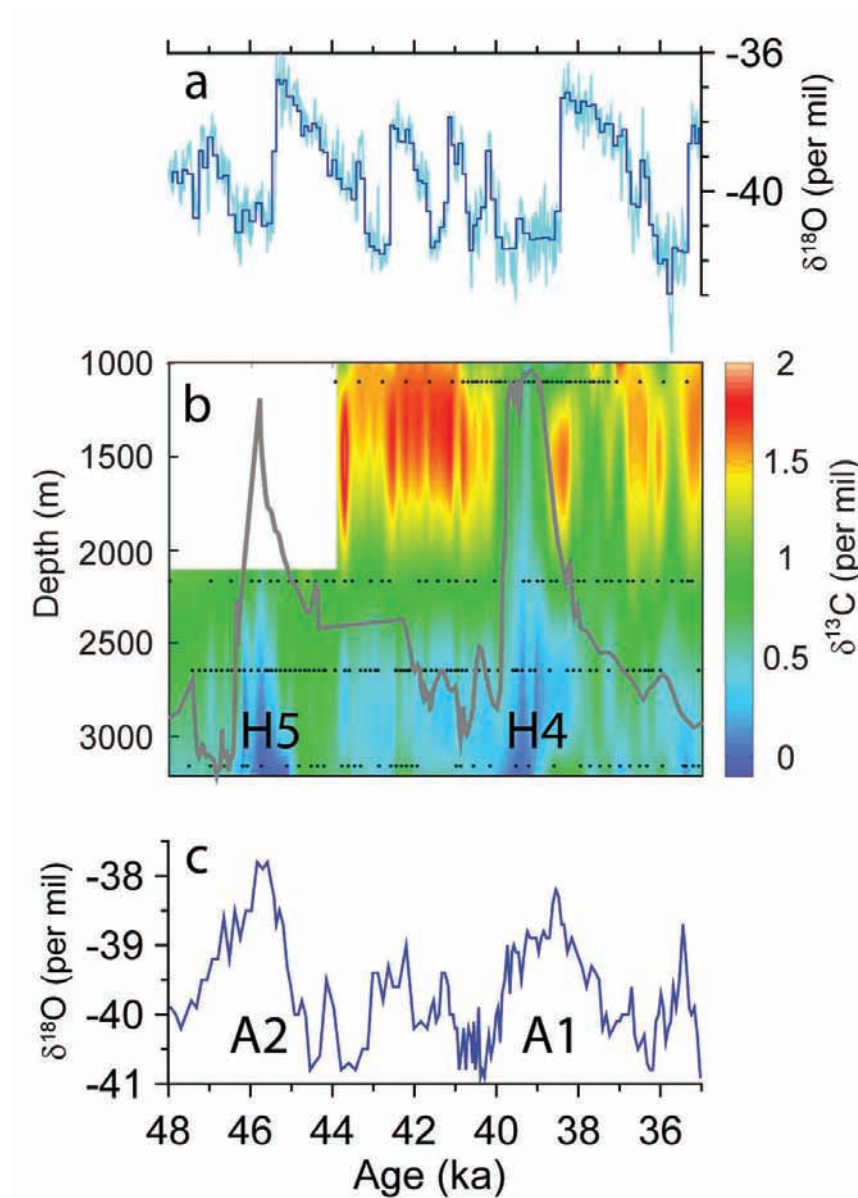
Figure 4.10. (a) The GISP2 δ^{18}O record (Grootes *et al.,* 1993; Stuiver and Grootes, 2000). Times of Heinrich events 4 and 5 identified (H4 and H5). (b) Time-varying δ^{13}C, a proxy for distribution of deep water masses, as a function of depth in the eastern North Atlantic based on four δ^{13}C records at water depths of 1,099 m (Zahn *et al.,* 1997), 2,161 m (Elliot *et al.,* 2002), 2,637 m (Skinner and Elderfield, 2007), and 3,146 m (Shackleton *et al.,* 2000). Control points from four cores used for interpolation are shown (black dots). More negative δ^{13}C values correspond to nutrient-rich Antarctic Bottom Water (AABW), whereas more positive δ^{13}C values correspond to nutrient-poor North Atlantic Deep Water (see Fig. 4.8). Also shown by the thick gray line is a proxy for Heinrich events, with peak values corresponding to Heinrich events H5 and H4 (Stoner *et al.,* 2000) (note that scale for this proxy is not shown). During Heinrich events H5 and H4, nutrient-rich AABW displaces NADW to shallow depths in the eastern North Atlantic basin. (c) The Byrd δ^{18}O record (Johnsen *et al.,* 1972), with the time scale synchronized to the GISP2 time scale by methane correlation (Blunier and Brook, 2001). ka, thousand years. A1, A2, Antarctic warm events.

changes in the North Atlantic water masses (and by inference the AMOC) during the D-O oscillations. These challenges include accurately dating and correlating sediment records beyond the reach of radiocarbon, and having low abundances of the appropriate species of benthic foraminifera in cores with high-enough resolution to distinguish the D-O oscillations.

In contrast to these difficulties in distinguishing and resolving D-O oscillations with water-mass tracers, the relative amount of magnetic minerals in deep-sea sediments in the path of the deep Atlantic overflows shows contemporaneous changes with all of the D-O oscillations (Kissel *et al.,* 1999). These magnetic minerals are derived from Tertiary basaltic provinces underlying the Norwegian Sea and are interpreted to record an increase (or decrease) in the velocity of the overflows from the Nordic Seas during D-O interstadials (or stadials). Taken at face value, the δ^{13}C and magnetic records may indicate that latitudinal shifts in the AMOC occurred, but with little commensurate change in the depth of deep water formation. The corresponding changes in the relative amount of magnetic minerals then reflect times when NADW formation occurred either in the Norwegian Sea, thus entraining magnetic minerals from the sea floor there, or in the open North Atlantic, at sites to the south of the source of the magnetic minerals. What remains unclear is whether changes in the overall strength of the AMOC accompanied these latitudinal shifts in NADW formation.

The fact that the global pattern of millennial-scale climate changes is consistent with that predicted from a weaker AMOC (see Sec. 6) has been taken as a strong indirect confirma-

tion that the stage 3 D-O oscillations are caused by AMOC changes (Alley, 2007; Clark *et al.,* 2007). However, care must be taken to separate the climate impacts of a much-reduced AMOC during Heinrich stadials, for which there is good evidence, from the non-Heinrich stadials, for which evidence of changes in the AMOC remains uncertain. This is often difficult in all but the highest resolution climate records. It has also been shown that changes in sea-ice concentrations in the North Atlantic can have a significant impact (Barnett *et al.,* 1989; Douville and Royer, 1996; Chiang *et al.,* 2003) and were likely involved in some of the millennial-scale climate variability during the deglaciation and stage 3 (Denton *et al.,* 2005; Li *et al.,* 2005; Masson-Delmotte *et al.,* 2005). Sea-ice changes may be a mechanism to amplify the impact of small changes in AMOC strength or location, but they may also result from changes in atmospheric circulation (Seager and Battisti, 2007).

4.6 Evidence for Changes in the AMOC during the Holocene

The proxy evidence for the state of the AMOC during the Holocene (0–11,500 years ago) is scarce and sometimes contradictory but clearly points to a more stable AMOC on millennial time scales than during the deglaciation or glacial times. Some δ^{13}C reconstructions suggest relatively dramatic changes in deep Atlantic water-mass properties on millennial time scales, but these changes are not always coherent between different sites (Oppo *et al.,* 2003; Keigwin *et al.,* 2005). Similarly, the δ^{13}C and trace-metal-based nutrient reconstructions on the same cores may disagree (Keigwin and Boyle, 2000). There is some indication from sediment grain size for variability in the strength of the overflows (Hall *et al.,* 2004), but the relatively constant flux of Pa/Th to the Atlantic sediments suggests only small changes in the AMOC (McManus *et al.,* 2004). The geostrophic reconstructions of the flow in the Florida Straits also suggest that small changes in the strength of the AMOC are possible over the last 1,000 years (Lund *et al.,* 2006).

There was a brief (about 150 year) cold snap in parts of the Northern Hemisphere at ~8,200 years ago, and it was proposed that this event may have resulted from a meltwater-

induced reduction in the AMOC (Alley and Agustdottir, 2005). There is now evidence of a weakening of the overflows in the North Atlantic from sediment grain size and magnetic properties (Ellison *et al.,* 2006; Kleiven *et al.,* 2008), and also a replacement of NADW (with high $\delta^{13}C$ ratios) by AABW (with low $\delta^{13}C$ ratios) in the deep North Atlantic (Kleiven *et al.,* 2008).

While many of the deep-sea sediment records are only able to resolve changes on millennial to centennial time scales, a recent study (Boessenkool *et al.,* 2007) reconstructs the strength of the Iceland-Scotland overflow on sub-decadal time scales over the last 230 years. This grain-size-based study suggests that the recent weakening over the last decades falls mostly within the range of its variability over the period of study. This work shows that paleoceanographic data may, in some locations, be used to extend the instrumental record of decadal- and centennial-scale variability.

4.7 Summary

We now have compelling evidence from a variety of paleoclimate proxies that the AMOC existed in a different state during the LGM, providing concrete evidence that the AMOC changed in association with the lower CO_2 and presence of the continental ice sheets. The LGM can be used to test the response of AMOC in coupled ocean atmosphere models to these changes (Sec. 5). We also have strong evidence for abrupt changes in the AMOC during the last deglaciation and during the Heinrich events, although the relation between these changes and known freshwater forcings is not always clear (Box 4.3). Better constraining both the magnitude and location of the freshwater perturbations that may have caused these changes in the AMOC will help to further refine the models, enabling better predictions of future abrupt changes in the AMOC. The relatively modest AMOC variability during the Holocene presents a challenge for the paleoclimate proxies and archives, but further progress in this area is important, as it will help establish the range of natural variability from which to compare any ongoing changes in the AMOC.

5. HOW WELL DO THE CURRENT COUPLED OCEAN-ATMOSPHERE MODELS SIMULATE THE OVERTURNING CIRCULATION?

Coupled ocean-atmosphere models are commonly used to make projections of how the AMOC might change in future decades. Confidence in these models can be improved by making comparisons of the AMOC both between models and between models and observational data. Even though the scarcity of observations presents a major challenge, it is apparent that significant mismatches are present and that continued efforts are needed to improve the skill of coupled models. This section reviews simulations of the present-day (Sec. 5.1), Last Glacial Maximum (Sec. 5.2), and transient events of the past (Sec. 5.3). Model projections of future changes in the AMOC are presented in Section 7.

5.1 Present-Day Simulations

A common model-model and model-data comparison uses the mean strength of the AMOC. Observational estimates are derived from either hydrographic data (Sec. 3.3; Ganachaud, 2003a; Talley *et al.,* 2003; Lumpkin and Speer, 2007) or inventories of chlorofluorocarbon tracers in the ocean (Smethie and Fine, 2001). The estimates are consistent with each other and suggest a mean overturning of about 15–18 Sv with errors of about 2–5 Sv.

Coupled atmosphere-ocean models using modern boundary conditions yield a wide range of values for overturning strength, which is usually defined as the maximum meridional overturning streamfunction value in the North Atlantic excluding the surface circulation. While the maximum overturning streamfunction is not directly observable, it is a very useful metric for model intercomparisons. Present-day control (*i.e.,* fixed forcing) simulations yield average AMOC intensities from model to model between 12 and 26 Sv (Fig. 4.11; Stouffer *et al.,* 2006), while simulations of the 20th century that include historical variations in forcing have a range from 10 to 30 Sv (Randall *et al.,*
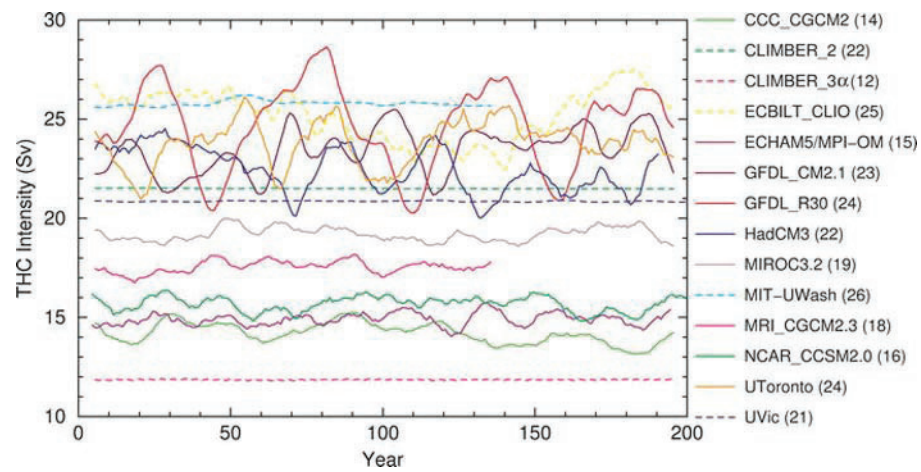
Figure 4.11. Time series of the strength of the Atlantic meridional overturning as simulated by a suite of coupled ocean-atmosphere models using present-day boundary conditions, from Stouffer *et al.* (2006). The strength is listed along the y-axis in Sverdrups (Sv; 1 Sv = 10^6 m^{3}s^{-1}). Curves were smoothed with a 10-yr running mean to reduce high-frequency fluctuations. The numbers after the model names indicate the long-term mean of the Atlantic MOC. THC, Thermohaline Circulation.

2007; see also Fig. 4.17). In addition, some of the 20th century simulations show substantial drifts that might hinder predictions of future AMOC strength (Randall *et al.,* 2007).

There are also substantial differences among models in AMOC variability, which tends to scale with the mean strength of the overturning. Models with a more vigorous overturning tend to produce pronounced multidecadal variations, while variability in models with a weaker AMOC is more damped (Stouffer *et al.,* 2006). Time series of the AMOC are too incomplete to give an indication of which mode is more accurate, although recent observations suggest that the AMOC is highly variable on sub-annual time scales (Sec. 3.3; Cunningham *et al.,* 2007).

Another useful model-data comparison can be made for ocean heat transport in the Atlantic. A significant fraction of the northward heat transport in the Atlantic is due to the AMOC, with additional contributions from horizontal circulations (*e.g.,* Roemmich and Wunsch, 1985). In the absence of variations in radiative forcing, changes in ocean heat storage are small when averaged over long periods. Under these conditions, ocean heat transport must balance surface heat fluxes, and the heat transport therefore provides an indication of how well surface fluxes are simulated. There are several calculations of heat transport at 20–25°N. in the Atlantic derived by combining hydro-

graphic observations in inverse models. These methods yield estimates of about 1.3 Petawatts (PW; 1 PW = 10^{15} Watts) with errors on the order of about 0.2 PW (Ganachaud and Wunsch, 2000; Stammer *et al.,* 2003). While all models agree that heat transport in the Atlantic is northward at 20°N., the modeled magnitude varies greatly (Fig. 4.12). Most models tend to underestimate the ocean heat transport, with ranges generally between 0.5 to 1.1 PW (Jia, 2003; Stouffer *et al.,* 2006). The mismatch is believed to result from two factors: (1) smaller than observed temperature differences between the upper and lower branches of the AMOC, with surface waters too cold and deep waters too warm, and (2) overturning that is too weak (Jia, 2003). The source of these model errors will be discussed further.

Schmittner *et al.* (2005) and Schneider *et al.* (2007) have proposed that the skill of a model in producing the climatological spatial patterns of temperature, salinity, and pycnocline depth in the North Atlantic is another useful measure of model ability to simulate the overturning circulation. These authors found that models simulate temperature better than salinity; they attribute errors in the latter to biases in the hydrologic cycle in the atmosphere (Schneider *et al.,* 2007). Large errors in pycnocline depth are probably the result of compounded errors from both temperature and salinity fields. Also, errors over the North Atlantic alone tend to be

significantly larger than those for the global field (Schneider *et al.,* 2007). Large cold biases of up to several degrees Celsius in the North Atlantic, seen in most coupled models, are attributed partly to misplacement of the Gulf Stream and North Atlantic Current and the large SST gradients associated with them (Randall *et al.,* 2007). Cold surface biases commonly contrast with temperatures that are about 2 °C too warm at depth in the region of North Atlantic Deep Water (Randall *et al.,* 2007).

Some of these model errors, particularly in temperature and heat transport, are related to the representation of western boundary currents (Gulf Stream and North Atlantic Current) and deep water overflow across the Greenland-Iceland-Scotland ridge. Two common model biases in the western boundary current are (1) a separation of the Gulf Stream from the coast of North America that occurs too far north of Cape Hatteras (Dengg *et al.,* 1996) and (2) a North Atlantic Current whose path does not penetrate the southern Labrador Sea, and is instead too zonal with too few meanders (Rossby, 1996). The effect of the first bias is to prohibit northward meanders and warm core eddies, negatively affecting heat transport and water mass transformation, while the second bias results in SSTs that are too cold. Both of these biases have been improved in standalone ocean models by increasing the resolution to about 0.1° so that mesoscale eddies may be resolved (*e.g.,* Smith *et al.,* 2000; Bryan *et al.,* 2007). The resolution of current coupled ocean-atmosphere models is typically on the order of 1° or more, requiring an increase in computing power of an order of magnitude before coupled ocean eddy-resolving simulations become routine. Initial results from coupling a high-resolution ocean model to an atmospheric model indicate that a corresponding increase in atmospheric resolution may also be necessary (Roberts *et al.,* 2004).

Ocean model resolution is also one of the issues involved in the representation of ocean convection, which can occur on very small spatial scales (Wadhams *et al.,* 2002) and in deep water overflows. Deep water masses

in the North Atlantic are formed in marginal seas and enter the open ocean through over-flows such as the Denmark Strait and the Faroe Bank Channel. Model simulations of overflows are unrealistic in several aspects, including (1) the specification of sill bathymetry, which is made difficult because the resolution is often too coarse to represent the proper widths and depths (Roberts and Wood, 1997), and (2) the representation of mixing of dense overflow waters with ambient waters downstream of the sill (Winton *et al.,* 1998). In many ocean models, topography is specified as discrete levels, which leads to a "stepped" profile descending from sills. Mixing of overflow waters with ambient waters occurs at each step, leading to excessive entrainment. As a result, deep waters in the lower branch of the AMOC are too warm and too fresh (*e.g.,* Tang and Roberts, 2005). Efforts are being made to improve this model deficiency through new parameterizations (Thorpe *et al.,* 2004; Tang and Roberts, 2005) or by using isopycnal or terrain-following vertical coordinate systems (Willebrand *et al.,* 2001).

Realistic simulation of sea ice is also important for the AMOC due to the effects of sea ice on the surface energy and freshwater budgets of the North Atlantic. The representation of dynamical and thermodynamical processes has become more sophisticated in the current generation of sea-ice models. Nevertheless, when coupled to atmosphere-ocean general circulation models, sea-ice models tend to yield unrealistically large sea-ice extents in the Northern Hemisphere,
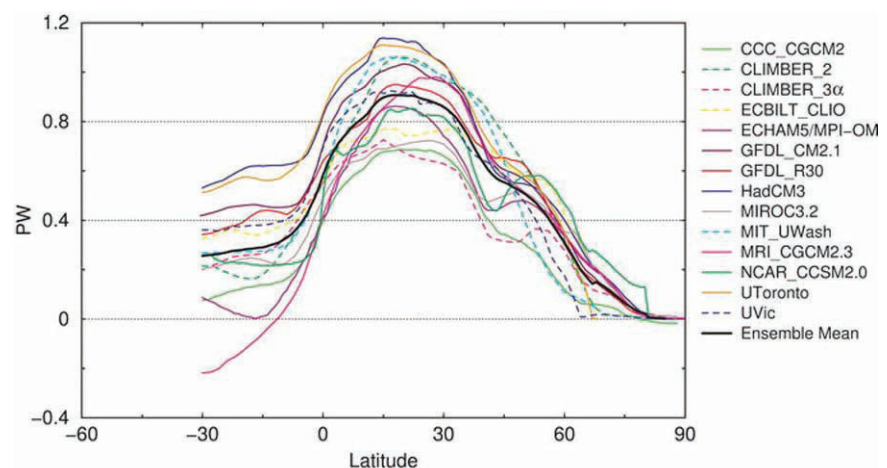

Figure 4.12. Northward heat transport in the Atlantic Ocean in an ensemble of coupled ocean-atmosphere models, from Stouffer *et al.* (2006). For comparison, observational estimates at 20–25°N. are about 1.3 ± 0.2 Petawatts (PW; 1 PW = 10^{15} Watts) (Ganachaud and Wunsch, 2000; Stammer *et al.,* 2003).

a poor simulation of regional distributions, and a large range in ice thickness (*e.g.,* Arzel *et al.,* 2006; Zhang and Walsh, 2006). These tendencies are the result of biases in winds, ocean mixing, and surface heat fluxes (Randall *et al.,* 2007).

5.2 Last Glacial Maximum Simulations

Characteristics of the overturning circulation at the LGM were reviewed in Section 3. Those that are the most robust and, therefore, the most useful for evaluating model performance are (1) a shallower boundary, at a level of about 2,000–2,500 m, between Glacial North Atlantic Intermediate Water and Antarctic Bottom Water (Duplessy *et al.,* 1988; Boyle, 1992; Curry and Oppo, 2005; Marchitto and Broecker, 2006); (2) a reverse in the north-south salinity gradient in the deep ocean to the Southern Ocean being much saltier than the North Atlantic (Adkins *et al.,* 2002); and (3) formation of Glacial North Atlantic Intermediate Water south of Iceland (Duplessy *et al.,* 1988; Sarnthein *et al.,* 1994; Pflaumann *et al.,* 2003).

It is more difficult to compare model results to inferred flow speeds, due to the lack of agreement among proxy records for this variable. Some studies suggest a vigorous circulation with transports not too different from today (McCave *et al.,* 1995; Yu *et al.,* 1996), while others suggest a decreased flow speed (Lynch-Stieglitz *et al.,* 1999; McManus *et al.,* 2004). All that can be said confidently is that there is no evidence for a significant strengthening of the overturning circulation at the LGM.

Results from LGM simulations are strongly dependent on the specified boundary conditions. In order to facilitate model-model and model-data comparisons, the second phase of the Paleoclimate Modelling Intercomparison Project (PMIP2; Braconnot *et al.,* 2007) coordinated a suite of coupled atmosphere-ocean model experiments using common boundary conditions. Models involved in this project include both General Circulation Models (GCMs) and Earth System Models of Intermediate Complexity (EMICs). LGM boundary conditions are known with varying degrees of certainty. Some are known well, including past insolation, atmospheric concentrations of greenhouse gases, and sea level. Others are known with less certainty,

including the topography of the ice sheets, vegetation and other land-surface characteristics, and freshwater fluxes from land. For these, PMIP2 simulations used best estimates (see Braconnot *et al.,* 2007). More work is necessary to narrow the uncertainty of these boundary conditions, particularly since some could have important effects on the AMOC.

PMIP2 simulations using LGM boundary conditions were completed with five models, three coupled atmosphere-ocean models and two EMICs. Only one of the models, the ECBilt-CLIO EMIC, employs flux adjustments. Although EMICs generally have not been included in future climate projections using multimodel ensembles, considering them within the context of model evaluation may yield additional understanding about how various model parameterizations and formulations affect the simulated AMOC.

The resulting AMOC in the the LGM simulations varies widely between the models, and several of the simulations are clearly not in agreement with the paleodata (Figs. 4.7, 4.13). A shoaling of the circulation is clear in only one of the models (the NCAR CCSM3); all other models show either a deepening or little change (Otto-Bliesner *et al.,* 2007; Weber *et al.,* 2007). Also, the north-south salinity gradient of the LGM deep ocean is not consistently reversed in these model simulations (Otto-Bliesner *et al.,* 2007). All models do show a southward shift of GNAIW formation, however. In general, the better the model matches one of these criteria, the better it matches the others as well (Weber *et al.,* 2007).

There is a particularly large spread among the models in terms of overturning strength (Fig. 4.13). Some models show a significantly increased AMOC streamfunction for the LGM compared to the modern control (by ~25–40%). Others have a significantly decreased streamfunction (by ~20–30%), while another shows very little change (Weber *et al.,* 2007). Again, the overturning strength is not constrained well enough from the paleodata to make this a rigorous test of the models. It is likely, though, that simulations with a significantly strengthened AMOC are not realistic, and this tempers the credibility of their projections of future

AMOC change. A more complete understanding of past AMOC changes and our ability to simulate those in models will lead to increased confidence in the projection of future changes.

Several factors control the AMOC response to LGM boundary conditions. These include changes in the freshwater budget of the North Atlantic, the density gradient between the North and South Atlantic, and the density gradient between GNAIW and AABW (Schmittner *et al.*, 2002; Weber *et al.*, 2007). The density gradient between GNAIW and AABW appears to be particularly important, and sea-ice concentrations have been shown to play a central role in determining this gradient (Otto-Bliesner *et al.*, 2007). The AMOC response also has some dependence on the accuracy of the control state. For example, models with an unrealistically shallow overturning circulation in the control simulation do not yield a shoaled circulation for LGM conditions (Weber *et al.*, 2007).

5.3 Transient Simulations of Past AMOC Variability

In addition to the equilibrium simulations discussed thus far, transient simulations of past meltwater pulses to the North Atlantic (see Sec. 4) may offer another test of model skill in simulating the AMOC. Such a test requires quantitative reconstructions of the freshwater pulse, including its volume, duration and location, plus the magnitude and duration of the resulting reduction in the AMOC. This information is not easy to obtain; coupled GCM simulations of most events, including the Younger Dryas and Heinrich events, have been forced with idealized freshwater pulses and compared with qualitative reconstructions of the AMOC (*e.g.*, Hewitt *et al.*, 2006; Peltier *et al.*, 2006). There is somewhat more information about the freshwater pulse associated with the 8.2 ka event, though important uncertainties remain (Clarke *et al.*, 2004; Meissner and Clark, 2006). A significant problem, however, is the scarcity of data about the AMOC during the 8.2 ka event. New ocean sediment records suggest the AMOC weakened following the freshwater pulse, but a quantitative reconstruction is lacking (Ellison *et al.*, 2006; Kleiven *et al.*, 2008). Thus, while simulations forced with the inferred freshwater pulse at 8.2 ka have produced results in quantitative agreement with reconstructed climate anomalies (*e.g.*, LeGrande *et al.*, 2006; Wiersma *et al.*, 2006), the 8.2 ka event is currently limited as a test of a model's ability to reproduce changes in the AMOC itself.
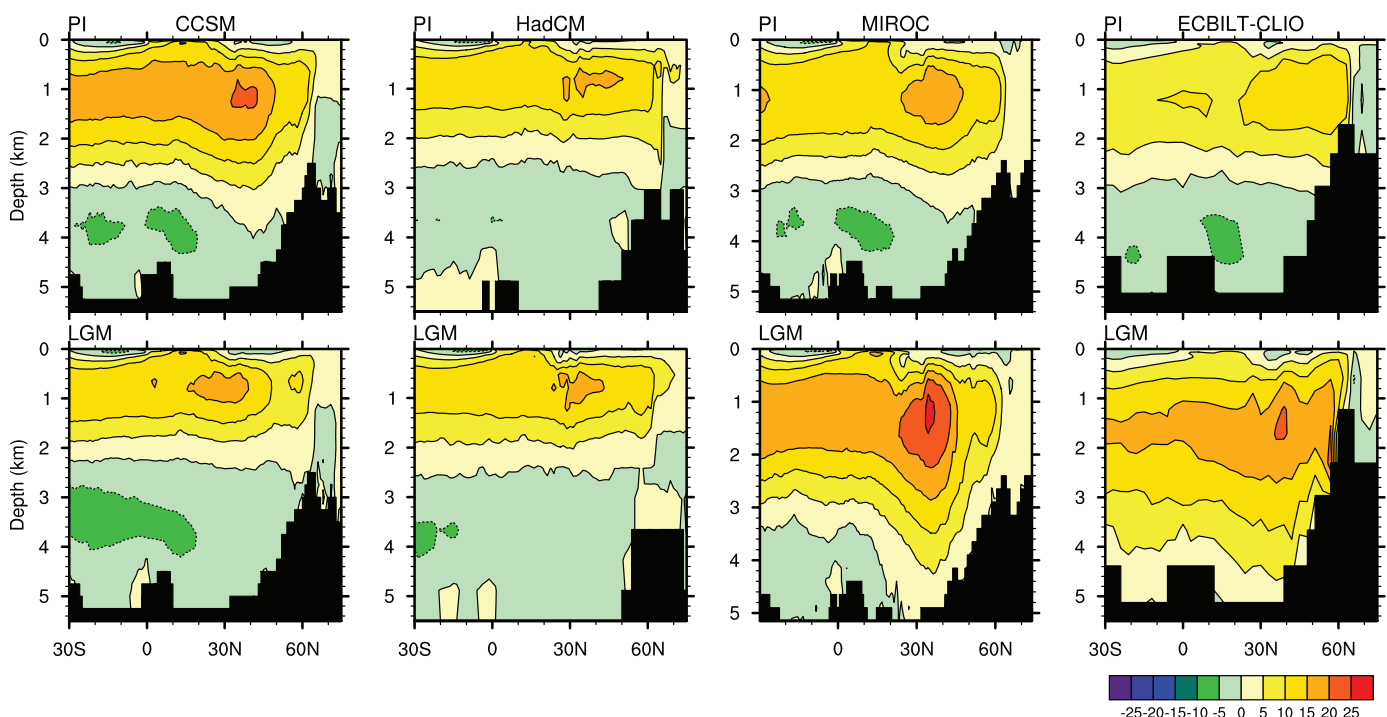

Figure 4.13. Atlantic meridional overturning (in Sverdrups) simulated by four PMIP2 coupled ocean-atmosphere models for modern (top) and the Last Glacial Maximum (bottom). From Otto-Bliesner *et al.* (2007).

6. WHAT ARE THE GLOBAL AND REGIONAL IMPACTS OF A CHANGE IN THE OVERTURNING CIRCULATION?

In this section we review some of the climatic impacts of the AMOC over a range of time scales. While all of the impacts are not necessarily abrupt, they indicate consistent physical relationships that might be anticipated with any abrupt change in the AMOC. We start with evidence of the climatic impact of AMOC changes during glacial periods. While AMOC changes are not hypothesized to cause Ice Ages, there are indications of large AMOC changes within glacial periods, and these offer excellent opportunities to evaluate the global-scale climatic impact of large AMOC changes. We then move on to possible impacts of AMOC changes during the instrumental era. All of these results point to global-scale, robust impacts of AMOC changes on the climate system. In particular, a central impact of AMOC changes is to alter the interhemispheric temperature gradient, thereby moving the position of the Intertropical Convergence Zone (ITCZ). Such ITCZ changes induce a host of regional climate impacts.

6.1 Extra-Tropical Impacts during the Last Ice Age

During the last glacial period, records indicate there were significant abrupt climate change events, such as the D-O oscillations and Heinrich events discussed in detail in Section 4. These are thought to be associated with changes in the AMOC, and thus offer important insights into the climatic impacts of large changes in the AMOC. The paleoproxies from the Bermuda

Rise (McManus *et al.,* 2004) further indicate that the AMOC was substantially weakened during the Younger Dryas cooling event and was almost shut down during the latest Heinrich event—H1. The AMOC transports a substantial amount of heat northward. A rapid shutdown of the AMOC causes a cooling in the North Atlantic and a warming in the South Atlantic, associated with the reduction of the northward ocean heat transport, as simulated by many climate models (Vellinga and Wood, 2002; Dahl *et al.,* 2005; Zhang and Delworth, 2005; Stouffer *et al.,* 2006).

The cooling stadials of the Greenland D-O oscillations were also synchronous with higher oxygen levels off the California coast (indicating reduced upwelling and reduced California Current) (Behl and Kennett, 1996), enhanced North Pacific intermediate-water formation, and the strengthening of the Aleutian Low (Hendy and Kennett, 2000). This teleconnection is seen in coupled modeling simulations in which the AMOC is suppressed in response to massive freshwater inputs (Mikolajewicz *et al.,* 1997; Zhang and Delworth, 2005), *i.e.,* cooling in the North Atlantic induced by a weakened AMOC can lead to the strengthening of the Aleutian Low and large-scale cooling in the central North Pacific.

The millennial-scale abrupt climate change events found in Greenland ice cores have been linked to the millennial-scale signal seen in Antarctic ice cores (Blunier *et al.,* 1998; Bender *et al.,* 1999; Blunier and Brook, 2001). A very recent high resolution glacial climate record derived from the first deep ice core in the Atlantic sector of the Southern Ocean region (Dronning Maud Land, Antarctica) shows a one-to-one coupling between all Antarctic warm events (*i.e.,* the A events discussed in detail in Sec. 3) and Greenland D-O oscillations during the last ice age (EPICA Community Members, 2006). The amplitude of the Antarctic warm events is found to be linearly dependent on the duration of the concurrent Greenland cooling events. Such a bipolar seesaw pattern was explained by changes in the heat flux connected to the reduction of the AMOC (Manabe and Stouffer, 1988; Stocker and Johnsen, 2003; EPICA Community Members, 2006).

6.2 Tropical Impacts During the Last Ice Age and Holocene

Recently, many paleorecords from different tropical regions have revealed abrupt changes that are remarkably coherent with the millennial-scale abrupt climate changes recorded in the Greenland ice cores during the glacial period, indicating that changes in the AMOC might have significant global-scale impacts on the tropics. A paleoproxy from the Cariaco basin off Venezuela suggests that the ITCZ shifted southward during cooling stadials of the Greenland D-O oscillations (Peterson *et al.,* 2000). Stott *et al.* (2002) suggest that Greenland cooling events were related to an El Niño-like pattern of sea surface temperature (SST) change, a weakened Walker circulation, and a southward shift of the ITCZ in the tropical Pacific. The tropical Pacific east-west SST contrast was further reduced during the latest Heinrich event (H1) and Younger Dryas event (Lea *et al.,* 2000; Koutavas *et al.,* 2002). Drying conditions in the northeastern tropical Pacific west of Central America were synchronous with the Younger Dryas and the latest Heinrich event—H1 (Benway *et al.,* 2006). When Greenland was in cooling condition, the summer Asian monsoon was reduced, as indicated by a record from Hulu Cave in eastern China (Wang *et al.,* 2001). Wet periods in northeastern Brazil are synchronous with Heinrich events, cold periods in Greenland, and periods of weak east Asian summer monsoons and decreased river runoff to the Cariaco basin (Wang *et al.,* 2004). Sediment records from the Oman margin in the Arabian Sea indicate that weakened Indian summer monsoon upwelling occurred during Greenland stadials (Altabet *et al.,* 2002).

The global synchronization of abrupt climate changes as indicated by these paleorecords, especially the anti-phase relationship of precipitation changes between the Northern Hemisphere (Hulu Cave in China, Cariaco basin) and the Southern Hemisphere (northeastern Brazil), is thought to be induced by changes in the AMOC. Global coupled climate models are employed to test this hypothesis. Figure 4.14 compares paleorecords with simulated changes in response to the weakening of the AMOC using the Geophysical Fluid Dynamics Laboratory (GFDL) coupled climate model (CM2.0). In the numerical experiment, the AMOC was

substantially weakened by freshening the high latitudes of the North Atlantic (Zhang and Delworth, 2005). This leads to a southward shift of the ITCZ over the tropical Atlantic (Fig. 4.14, upper right), similar to that found in many modeling studies (Vellinga and Wood, 2002; Dahl *et al.,* 2005; Stouffer *et al.,* 2006). This southward shift of the Atlantic ITCZ is consistent with paleorecords of drier conditions over the Cariaco basin (Peterson *et al.,* 2000) and wetter conditions over northeastern Brazil during Heinrich events (Wang *et al.,* 2004) (Fig. 4.14, lower right). Beyond the typical responses in the Atlantic, this experiment also shows many significant remote responses outside the Atlantic, such as a southward shift of the ITCZ in the tropical Pacific (Fig. 4.14, upper right), consistent with drying conditions over the northeastern tropical Pacific during the Younger Dryas and Heinrich events (Benway *et al.,* 2006). The modeled weakening of the Indian and East Asian summer monsoon in response to the weakening of the AMOC (Fig. 4.14, upper left) is also consistent with paleoproxies from the Indian Ocean (Altabet *et al.,* 2002; Fig. 4.14, lower left) and the Hulu Cave in eastern China (Wang *et al.,* 2001, 2004; Fig. 4.14, lower right). The simulated weakening of the AMOC also led to reduced cross-equatorial and east-west SST contrasts in the tropical Pacific, an El Niño-like condition, and a weakened Walker circulation in the southern tropical Pacific, a La Niña-like condition, and a stronger Walker circulation in the northern tropical Pacific. Coupled air-sea interactions and ocean dynamics in the tropical Pacific are important for connecting the Atlantic changes with the Asian monsoon variations (Zhang and Delworth, 2005). Thus, both atmospheric teleconnections and coupled air-sea interactions play crucial roles for the global-scale impacts of the AMOC.

Similar global-scale synchronous changes on a multidecadal to centennial time scale have also been found during the Holocene. For example, the Atlantic ITCZ shifted southward during the Little Ice Age and northward during the Medieval Warm Period (Haug *et al.,* 2001). Sediment records in the anoxic Arabian Sea show that centennial-scale Indian summer monsoon variability coincided with changes in the North Atlantic region during the Holocene, including a weaker summer monsoon during the Little Ice

Many paleorecords from different tropical regions have revealed abrupt changes that are remarkably coherent with the millennial-scale abrupt climate changes recorded in the Greenland ice cores during the glacial period, indicating that changes in the AMOC might have significant global-scale impacts on the tropics.
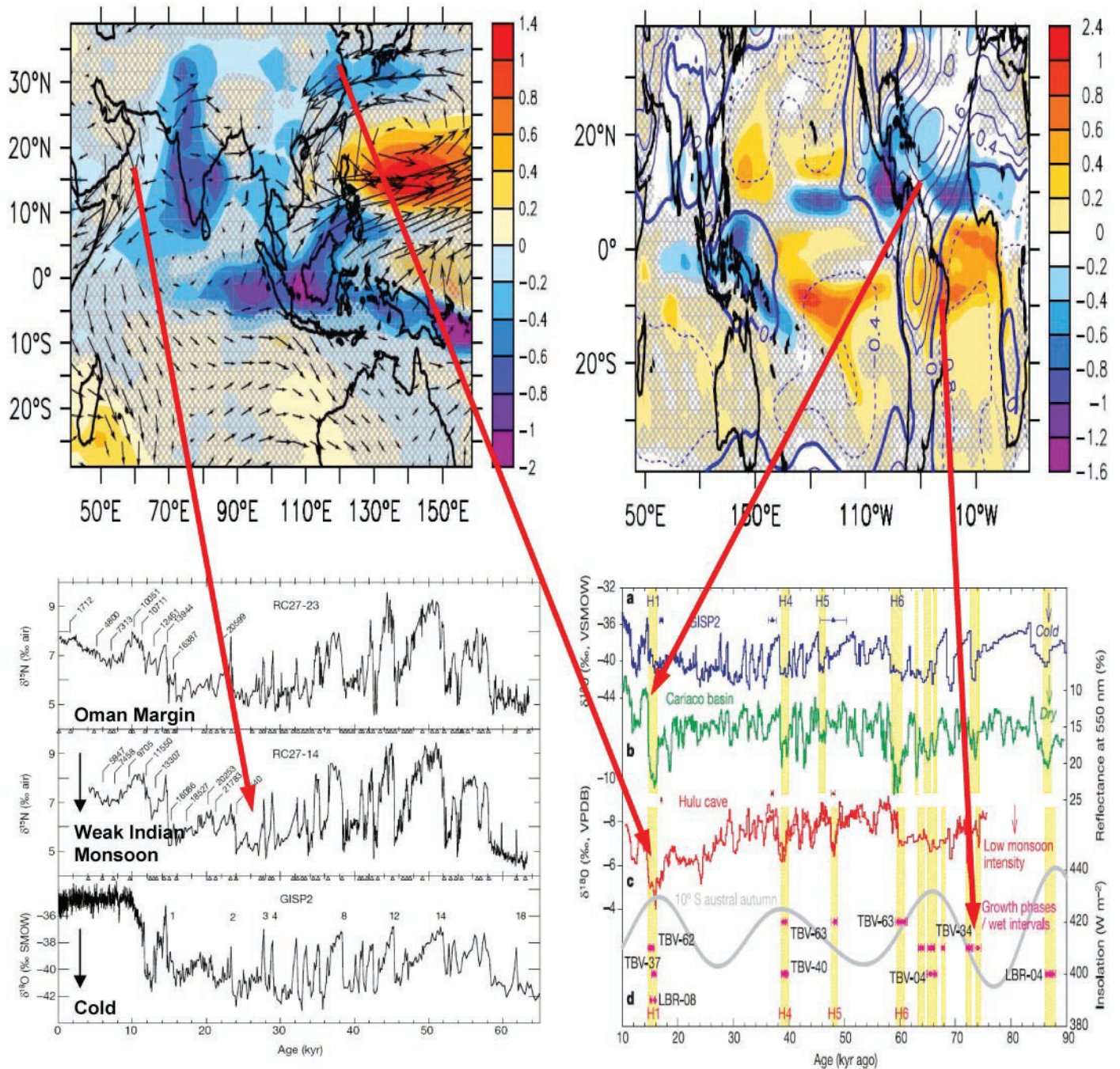
Figure 4.14. Comparison of simulated changes in response to the weakening of the AMOC using the Geophysical Fluid Dynamics Laboratory (GFDL) coupled model (CM2.0) with paleorecords. Upper left (from Zhang and Delworth, 2005; used with permission, copyright 2005, American Meterological Society): Simulated summer precipitation change (color shading, units are m yr^{-1}) and surface wind change (black vectors) over the Indian and eastern China regions. Upper right (Zhang and Delworth, 2005): Simulated annual mean precipitation change (color shading, units are m yr^{-1}) and sea-level pressure change (contour, units are hPa). Negative values correspond to a reduction of precipitation. Lower left (Altabet *et al.,* 2002): The δ^{15}N records for denitrification from sediment cores from the Oman margin in the Arabian Sea were synchronous with D-O oscillations recorded in Greenland ice cores (GISP2) during the last glacial period, *i.e.,* the reduced denitrification, indicating weakened Indian summer monsoon upwelling, occurred during cold Greenland stadials. Lower right (Wang *et al.,* 2004): Comparison of the growth patterns of speleothems from northeastern Brazil (d) with (a) δ^{18}O values of Greenland ice cores (GISP2), (b) Reflectance of the Cariaco basin sediments from ODP Hole 1002C (Peterson *et al.,* 2000), (c) δ^{18}O values of Hulu cave stalagmites (Wang *et al.,* 2001; used with permission from *Science*). The modeled global response to the weakening of the AMOC (Zhang and Delworth, 2005) is consistent with all these synchronous abrupt climate changes found from the Oman margin, Hulu Cave, Cariaco basin, and northeastern Brazil during cold Greenland stadials, *i.e.,* drying at the Cariaco basin, weakening of the Indian and Asian summer monsoon, and wetting in northeastern Brazil (red arrows). Abbreviations: %, percent; ‰, per mil; SMOW, Standard Mean Ocean Water; kyr, thousand years ago; H1, H4, H5, H6, Heinrich events; W m^{-2}, watts per square meter; nm, nanometer; m yr^{-1}, meters per year; hPa, hectoPascals.

Age and an enhanced summer monsoon during the Medieval Warm Period (Gupta *et al.,* 2003). These changes might also be associated with a reduction of the AMOC during the Little Ice Age (Lund *et al.,* 2006).

6.3 Possible Impacts During the 20th Century

Instrumental records in the 20th century can also provide clues about possible AMOC impacts. Instrumental records show significant large-scale multidecadal variations in the Atlantic SST. The observed detrended 20th century multidecadal SST anomaly averaged over the North Atlantic, often called the Atlantic Multi-decadal Oscillation (AMO) (Enfield *et al.,* 2001; Knight *et al.,* 2005), has significant regional and hemispheric climate impacts (Enfield *et al.,* 2001; Knight *et al.,* 2006; Zhang and Delworth, 2006; Zhang *et al.,* 2007a). The warm AMO phases occurred during 1925–65 and the recent decade since 1995, and cold phases occurred during 1900–25 and 1965–95. The AMO index is highly correlated with multidecadal variations of the tropical North Atlantic (TNA) SST and Atlantic hurricane activity (Goldenberg *et al.,* 2001; Landsea, 2005; Knight *et al.,* 2006; Zhang and Delworth, 2006; Sutton and Hodson, 2007). The observed TNA surface warming is correlated with above-normal Atlantic hurricane activity during the 1950–60s and the recent decade since 1995.

While the origin of these multidecadal SST variations is not certain, one leading hypothesis involves fluctuations of the AMOC. Models provide some support for this (Delworth and Mann, 2000; Knight *et al.,* 2005), with typical AMOC variability of several Sverdrups on multidecadal time scales, corresponding to 5–10% of the mean in these models. Another hypothesis is that they are forced by changes in radiative forcing (Mann and Emanuel, 2006). Delworth *et al.* (2007) suggest that both processes—radiative forcing changes, along with internal variability, possibly associated with the AMOC—may be important. A very recent study (Zhang, 2007) lends support to the hypothesis that AMOC fluctuations are important for the multidecadal variations of observed TNA SSTs. Zhang (2007) finds that observed TNA SST is strongly anticorrelated with TNA subsurface ocean temperature (after removing

long-term trends). This anticorrelation is a distinctive signature of the AMOC variations in coupled climate models; in contrast, simulations driven by external radiative forcing changes do not generate anticorrelated surface and subsurface TNA variations, lending support to the idea that the observed TNA SST fluctuations may be AMOC-induced.

6.3.1 Tropical Impacts

Empirical analyses have demonstrated a link between multidecadal fluctuations of Atlantic sea surface temperatures and Sahelian (African) summer rainfall variations (Folland *et al.,* 1986), in which an unusually warm North Atlantic is associated with increased summer rainfall over the Sahel. Studies with atmospheric general circulation models (*e.g.,* Giannini *et al.,* 2003; Lu and Delworth, 2005) have shown that models, when given the observed multidecadal SST variations, are able to reproduce much of the observed Sahelian rainfall variations. However, these studies do not identify the source of the SST fluctuations. Recent work (Held *et al.,* 2005) suggests that increasing greenhouse gases and aerosols may also be important factors in the late 20th century Sahelian drying.

The source of the observed Atlantic multidecadal SST variations has not been firmly established. One leading candidate mechanism involves fluctuations of the AMOC. Knight *et al.* (2006) have analyzed a 1,400-year control integration of the coupled climate model HADCM3 and found a clear relationship between AMO-like SST fluctuations and surface air temperature over North America and Eurasia, modulation of the vertical shear of the zonal wind in the tropical Atlantic, and large-scale changes in Sahel and Brazil rainfall. Linkages between the AMO and these tropical variations were often based on statistical analyses. Linkages between AMOC changes and tropical conditions, emphasizing the importance of changes in the atmospheric and oceanic energy budgets, are emphasized in Cheng *et al.* (2007). To investigate the causal link between the AMO and other multidecadal variability, Zhang and Delworth (2006) simulated the impact of AMO-like SST variations on climate with a hybrid coupled model. They demonstrated that many features of observed
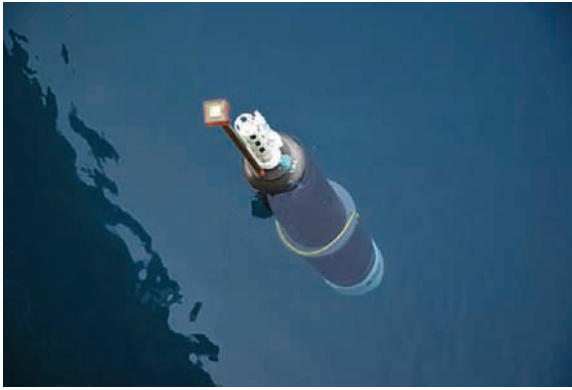
multidecadal climate variability in the 20th century may be interpreted—at least partially—as a response to the AMO. A warm phase of the AMO leads to a northward shift of the Atlantic ITCZ, and thus an increase in the Sahelian and Indian summer monsoonal rainfall, as well as a reduction in the vertical shear of the zonal wind in the tropical Atlantic region that is important for the development of Atlantic major Hurricanes (Fig. 4.15). Thus, the AMO creates large-scale atmospheric circulation anomalies that would be favorable for enhanced tropical storm activity. The study of Black *et al.* (1999) using Caribbean sediment records suggests that a southward shift of the Atlantic ITCZ when the North Atlantic is cold—similar to what is seen in the models—has been a robust feature of the climate system for more than 800 years, and is similar to results from the last ice age.

6.3.2 Impacts on North America and Western Europe

The recent modeling studies (Sutton and Hodson, 2005, 2007) provide a clear assessment of the impact of the AMO over the Atlantic, North America, and Western Europe (Fig. 4.16). In response to a warm phase of the AMO, a broad area of low pressure develops over the Atlantic, extending westward into the Caribbean and Southern United States. The pressure anomaly pattern denotes weakened easterly trade winds, potentially reinforcing the positive SST anomalies in the tropical North Atlantic Ocean by reducing the latent heat flux. Precipitation is generally enhanced over the warmer Atlantic waters and is reduced over a broad expanse of the United States. The summer temperature response is clear, with substantial warming over the United States and Mexico, with weaker warming over Western Europe.

Observational analyses (Enfield *et al.,* 2001) suggest that the AMO has a strong impact on the multidecadal variability of U.S. rainfall and river flows. McCabe *et al.* (2004) further suggest that there is significant positive correlation between the AMO and the Central U.S. multidecadal drought frequency, and the positive AMO phase contributes to the droughts observed over the continental U.S. in the decade since 1995.

6.3.3 Impacts on Northern Hemisphere Mean Temperature

Knight *et al.* (2005) find in the 1,400-year control integration of the HADCM3 climate model that variations in the AMOC are correlated with variations in the Northern Hemisphere mean surface temperature on decadal and longer time scales. Zhang *et al.* (2007a) demonstrate that AMO-like SST variations can contribute to the Northern Hemispheric mean surface temperature fluctuations, such as the early 20th century warming, the pause in hemispheric-scale warming in the mid-20th century, and the late 20th century rapid warming, in addition to the long-term warming trend induced by increasing greenhouse gases.

6.4 Simulated Impacts on ENSO Variability

Modeling studies suggest that changes in the AMOC can modulate the characteristics of El-Niño Southern Oscillation (ENSO). Timmermann *et al.* (2005a) found that the simulated weakening of the AMOC leads to a deepening of the tropical Pacific thermocline, and a weakening of ENSO, through the propagation of oceanic waves from the Atlantic to the tropical Pacific. Very recent modeling studies (Dong and Sutton, 2007; Timmermann *et al.,* 2007) found opposite results, *i.e.,* the weakening of the AMOC leads to an enhanced ENSO variability through atmospheric teleconnections. Dong *et al.* (2006) also show that a negative phase of the AMO leads to an enhancement of ENSO variability.

6.5 Impacts on Ecosystems

Recent coupled climate–ecosytem model simulations (Schmittner, 2005) find that a collapse of the AMOC leads to a reduction of North Atlantic plankton stocks by more than 50%, and
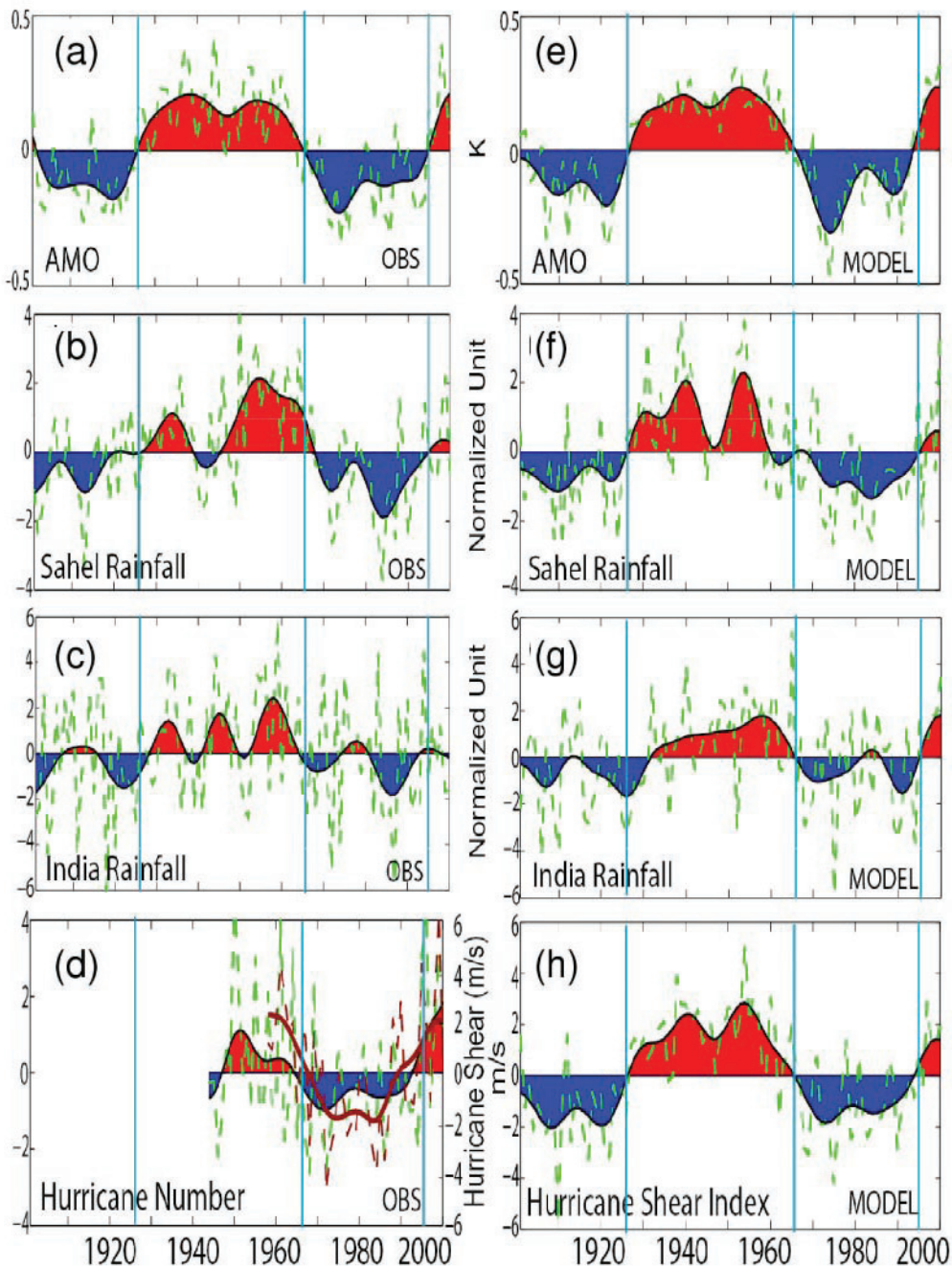
Figure 4.15. Left: various observed (OBS) quantities with an apparent association with the AMO. Right: Simulated responses of various quantities to AMO-like fluctuations in the Atlantic Ocean from a hybrid coupled model (adapted from Zhang and Delworth, 2006). Dashed green lines are unfiltered values, while the red and blue color-shaded values denote low-pass filtered values. Blue shaded regions indicate values below their long-term mean, while red shading denotes values above their long-term mean. The vertical blue lines denote transitions between warm and cold phases of the AMO. Time in calendar years is along the bottom axis. (a), (e) AMO Index, a measure of SST over the North Atlantic. Positive values denote an unusually warm North Atlantic. (b), (f) Normalized summer rainfall anomalies over the Sahel (20°W.–40°E.,10–20°N.). (c), (g) Normalized summer rainfall over west-central India (65–80°E.,15–25°N.). (d) Number of major Atlantic Hurricanes from the NOAA HURDAT data set. The brown lines denote the vertical shear of the zonal (westerly) wind (multiplied by –1) derived from the ERA-40 reanalysis, *i.e.,* the difference in the zonal wind between 850 and 200 hectopascals (hPa) over the south-central part of the main development region (MDR) for tropical storms (10–14°N.,70–20°W.). (h) Vertical shear of the simulated zonal wind (multiplied by –1), calculated as in (d).
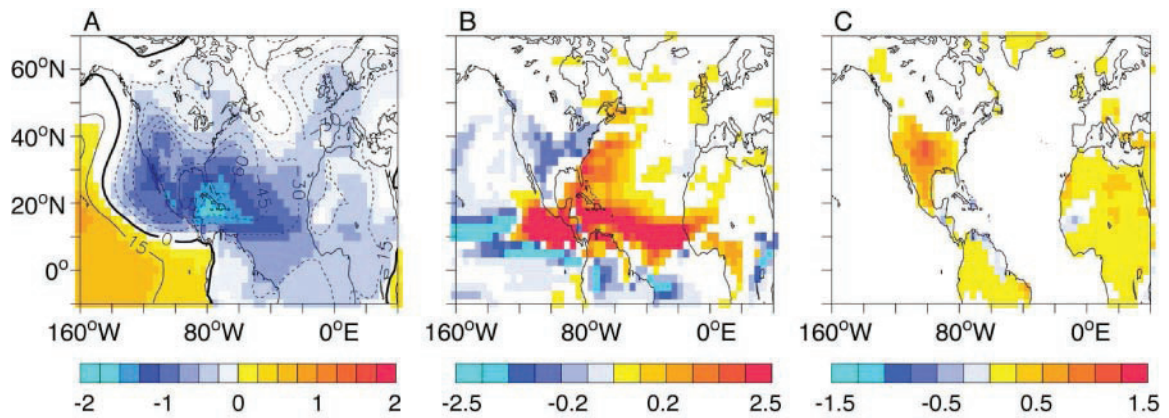
Figure 4.16. These panels (adapted from Sutton and Hodson, 2005; used with permission from *Science*) show the simulated response of various fields to an idealized AMO SST anomaly using the HADAM3 Atmospheric General Circulation Model. Results are time means for the August–October period. (a) Sea level pressure, units are pascals (Pa), with an interval of 15 Pa. (b) Precipitation, units are millimeters per day. (c) Surface air temperature, units are kelvin.

a reduction of global productivity by about 20% due to reduced upwelling of nutrient-rich deep water and depletion of upper ocean nutrient concentrations. The model results are consistent with paleorecords during the last ice age indicating low productivity during Greenland cold stadials and high productivity during Greenland warm interstadials (Rasmussen *et al.,* 2002). Multidecadal variations in abundance of Norwegian spring-spawning herring (a huge pelagic fish stock in the northeast Atlantic) have been found during the 20th century. These variations of the Atlantic herring are in phase with the AMO index and are mainly caused by variations in the inflowing Atlantic water temperature (Toresen and Østvedt, 2000). Model simulations show that the stocks of Arcto-Norwegian cod could decrease substantially in reaction to a weakened AMOC (Vikebø *et al.,* 2007). Further, Schmittner *et al.* (2007) show that changes in Atlantic circulation can have large effects on marine ecosystems and biogeochemical cycles, even in areas remote from the Atlantic, such as the Indian and North Pacific Oceans.

6.6 Summary and Discussion

A variety of observational and modeling studies demonstrate that changes in the AMOC induce a near-global-scale suite of climate system changes. A weakened AMOC cools the North Atlantic, leading to a southward shift of the ITCZ, with associated drying in the Caribbean, Sahel region of Africa, and the Indian and Asian monsoon regions. Other near-global-scale impacts include modulation of the Walker circulation and associated air-sea interactions in the Pacific basin, possible impacts on North American drought, and an imprint on hemispheric mean surface air temperatures. These relationships appear robust across a wide range of time scales, from observed changes in the 20th century to changes inferred from paleoclimate indicators from the last ice age climate.

In addition to the above impacts, regional changes in sea level would accompany a substantial change in the AMOC. For example, in simulations of a collapse of the AMOC (Levermann *et al.,* 2005; Vellinga and Wood, 2007), there is a sea level rise of up to 80 cm in the North Atlantic. This sea level rise is a dynamic effect associated with changes in ocean circulation. This would be in addition to other global warming induced changes in sea level arising from large-scale warming of the global ocean and melting of land-based ice sheets induced by increasing CO_2. This additional sea level rise could affect the coastlines of the United States, Canada, and Europe.

A weakened AMOC cools the North Atlantic, leading to a southward shift of the ITCZ, with associated drying in the Caribbean, Sahel region of Africa, and the Indian and Asian monsoon regions.

7. WHAT FACTORS THAT INFLUENCE THE OVERTURNING CIRCULATION ARE LIKELY TO CHANGE IN THE FUTURE, AND WHAT IS THE PROBABILITY THAT THE OVERTURNING CIRCULATION WILL CHANGE?

As noted in the Intergovernmental Panel for Climate Change (IPCC) Fourth Assessment Report (AR4), all climate model projections under increasing greenhouse gases lead to an increase in high-latitude temperature as well as an increase in high-latitude precipitation (Meehl *et al.,* 2007). Both warming and freshening tend to make the high-latitude surface waters less dense, thereby increasing their stability and inhibiting convection.

In the IPCC AR4, 19 coupled atmosphere-ocean models contributed projections of future climate change under the SRES A1B scenario (Meehl *et al.,* 2007). Of these, 16 models did not use flux adjustments (all except CGCM3.1, INM-CM3.0, and MRI-CGCM2.3.2). In making their assessment, Meehl *et al.* (2007) noted that several of the models simulated a late 20th century AMOC strength that was inconsistent with present-day estimates: 14–18 Sv at 24°N. (Ganachaud and Wunsch, 2000; Lumpkin and Speer, 2003); 13–19 Sv at 48°N. (Ganachaud, 2003a); maximum values of 17.2 Sv (Smethie and Fine, 2001) and 18 Sv (Talley *et al.,* 2003) with an error of ± 3–5 Sv. As a consequence of their poor 20th century simulations, these models were not used in their assessment.

The full range of late 20th century estimates of the Atlantic MOC strength (12–23 Sv) is spanned by the model simulations (Fig. 4.17; Schmittner *et al.,* 2005; Meehl *et al.,* 2007). The models further project a decrease in the AMOC strength of between 0% and 50%, with a multimodel average of 25%, over the course of the 21st century. None of the models simulated an abrupt shutdown of the AMOC during the 21st century.

Schneider *et al.* (2007) extended the analysis of Meehl *et al.* (2007) by developing a multi-model average in which the individual model simulations were weighted a number of ways. The various weighting estimates were based on an individual model's simulation of the contemporary ocean climate, and in particular its simulated fields of temperature, salinity, pycnocline depth, as well as its simulated Atlantic MOC strength. Their resulting best estimate 21st century AMOC weakening of 25–30% was invariant to the weighting scheme used and is consistent with the simple multimodel mean of 25% obtained in the IPCC AR4.

In early versions of some coupled atmosphere-ocean models, (*e.g.,* Dixon *et al.,* 1999), increased high-latitude precipitation dominated over increased high-latitude warming in causing the projected weakening of the AMOC under increasing greenhouse gases, while in others (*e.g.,* Mikolajewicz and Voss, 2000), the opposite was found. However, Gregory *et al.* (2005) undertook a recent model intercomparison project in which, in all 11 models analyzed, the AMOC reduction was caused more by changes in surface heat flux than changes in surface freshwater flux. Weaver *et al.* (2007) extended this analysis by showing that, in one model, this conclusion was independent of the initial mean climate state.

A number of stabilization scenarios have been examined using both coupled Atmosphere-Ocean General Circulation Models (AOGCMs) (Stouffer and Manabe, 1999; Voss and Mikolajewicz, 2001; Stouffer and Manabe, 2003; Wood *et al.,* 2003; Yoshida *et al.,* 2005; Bryan *et al.,* 2006) as well as Earth System Models of Intermediate Complexity (EMICs) (Meehl *et al.,* 2007). Typically the atmospheric CO_2 concentration in these models is increased at a rate of 1%/year to either two times or four times the preindustrial level of atmospheric CO_2, and held fixed thereafter. In virtually every simulation, the AMOC reduces but recovers to its initial strength when the radiative forcing is stabilized at two times or four times the preindustrial levels of CO_2. Only one early flux-adjusted model simulated a complete shutdown, and even this was not permanent (Manabe and Stouffer, 1994; Stouffer and Manabe, 2003). The only model to exhibit a permanent cessation of the AMOC in response to increasing greenhouse gases was an intermediate complexity model which incorporates a zonally averaged ocean component (Meehl *et al.,* 2007).
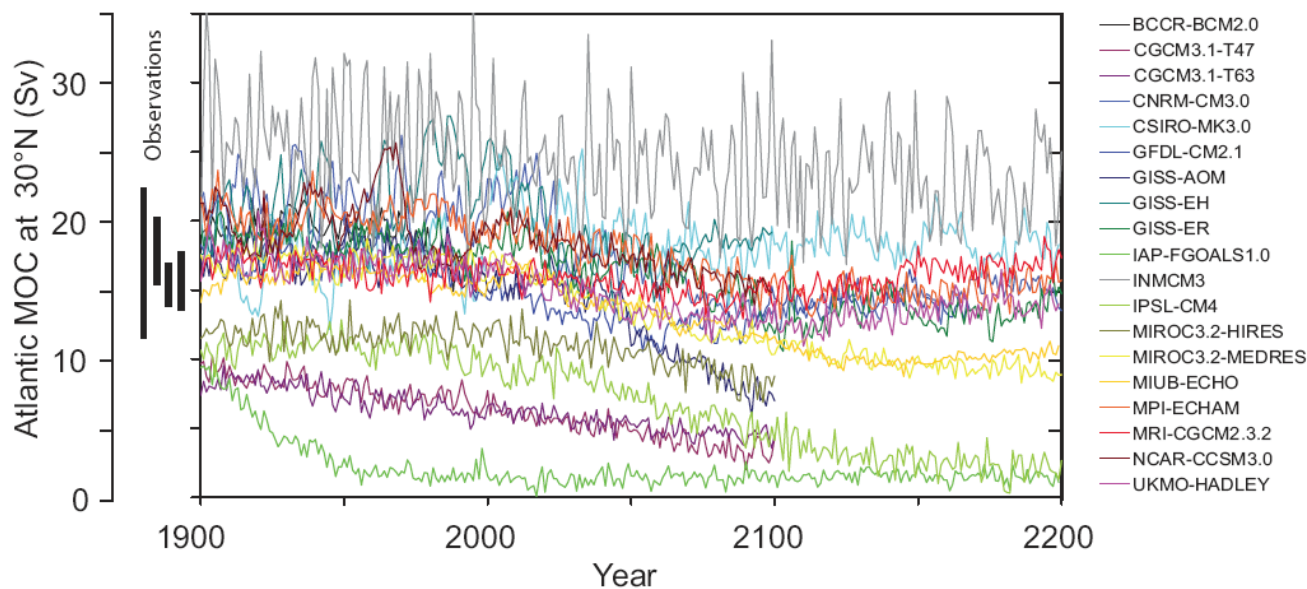
Figure 4.17. The Atlantic meridional overturning circulation (AMOC) at 30°N from the 19 coupled atmosphere-ocean models assessed in the IPCC AR4. The SRES A1B emissions scenario was used from 1999 to 2100. Those model projections that continued to 2200 retained the year 2100 radiative forcing for the remainder of the integration. Observationally based estimates of the late 20th century AMOC strength are also shown on the left as black bars. Taken from Meehl *et al.* (2007) as originally adapted from Schmittner *et al.* (2005).

Historically, coupled models that eventually lead to a collapse of the AMOC under global warming conditions were of lower resolution, used less complete physics, used flux adjustments, or were models of intermediate complexity with zonally averaged ocean components (wherein convection and sinking of water masses are coupled). The newer models assessed in the IPCC AR4 typically do not involve flux adjustments and have more stable projections of the future evolution of the AMOC.

One of the most misunderstood issues concerning the future of the AMOC under anthropogenic climate change is its often cited potential to cause the onset of the next ice age (see Box 4.4). A relatively solid understanding of glacial inception exists wherein a change in seasonal incoming solar radiation (warmer winters and colder summers), which is associated with changes in the Earth's axial tilt, longitude of perihelion, and the precession of its elliptical orbit around the sun, is required. This small change must then be amplified by albedo feedbacks associated with enhanced snow and ice cover, vegetation feedbacks associated with the expansion of tundra, and greenhouse gas feedbacks associated with the uptake (not

release) of carbon dioxide and reduced release or increased destruction rate of methane. As discussed by Berger and Loutre (2002) and Weaver and Hillaire-Marcel (2004a,b), it is not possible for global warming to cause an ice age.

Wood *et al.* (1999), using HADCM3 with sufficient resolution to resolve Denmark Strait overflow, performed two transient simulations starting with a preindustrial level of atmospheric CO_2 and subsequently increasing it at a rate of 1% or 2% per year. Convection and overturning in the Labrador Sea ceased in both these experiments, while deep water formation persisted in the Nordic seas. As the climate warmed, the Denmark Strait overflow water became warmer and hence lighter, so that the density contrast between it and the deep Labrador Sea water (LSW) was reduced. This made the deep circulation of the Labrador Sea collapse, while Denmark Strait overflow remained unchanged, a behavior suggested from the paleoreconstructions of Hillaire-Marcel *et al.* (2001) for the Last Interglacial (Eemian). The results of Hillaire-Marcel *et al.* (2001) suggest that the modern situation, with active LSW formation, has apparently no analog throughout the last glacial cycle, and thus appears a feature exclusive to the present interglacial.

One of the most misunderstood issues concerning the future of the AMOC under anthropogenic climate change is its often cited potential to cause the onset of the next ice age.

Results similar to those of Wood *et al.* (1999) were found by Hu *et al.* (2004), although Hu *et al.* (2004) also noted a significant increase in Greenland-Iceland-Norwegian (GIN) Sea convection as a result of enhanced inflow of saline North Atlantic water, and reduced outflow of sea ice from the Arctic. Some coupled models, on the other hand, found significant reductions in convection in the GIN Sea in response to increasing atmospheric greenhouse gases (Bryan *et al.,* 2006; Stouffer *et al.,* 2006). A cessation of LSW formation by 2030 was also found in high-resolution ocean model simulations of the Atlantic Ocean driven by surface fluxes from two coupled atmosphere-ocean climate models (Schweckendiek and Willebrand, 2005). Cottet-Puinel *et al.* (2004) obtained similar results to Wood *et al.* (1999) concerning the transient cessation of LSW formation and further showed that LSW formation eventually reestablished upon stabilization of anthropogenic greenhouse gas levels. The same model experiments of Wood *et al.* (1999) suggest that the freshening North Atlantic surface waters presently observed (Curry *et al.,* 2003) is associated with a transient increase of the AMOC (Wu *et al.,* 2004). Such an increase would be consistent with findings of Latif *et al.* (2006), who argued that their analysis of ocean observations and model simulations supported the notion of a slight AMOC strengthening since the 1980s.

The best estimate of sea level rise from 1993 to 2003 associated with mass loss from the Greenland ice sheet is 0.21 ± 0.07 mm yr^{-1} (Bindoff *et al.,* 2007). This converts to only 0.0015 to 0.0029 Sv of freshwater forcing, an amount that is too small to affect the AMOC in models (see Weaver and Hillaire-Marcel, 2004a; Jungclaus *et al.,* 2006). Recently, Velicogna and Wahr (2006) analyzed the Gravity Recovery and Climate Experiment (GRACE) satellite data to infer an acceleration of Greenland ice loss from April 2002 to April 2006 corresponding to 0.5 ± 0.1 mm/yr of global sea level rise. The equivalent 0.004–0.006 Sv of freshwater forcing is, once more, too small to affect the AMOC in models. Stouffer *et al.* (2006) undertook an intercomparison of 14 coupled models subject to a 0.1-Sv freshwater perturbation (17 times the upper estimate from GRACE data) applied for 100 years to the northern North Atlantic Ocean. A simple scaling analysis (conducted by the authors of this assessment report) shows that if over a 10-year period Arctic sea ice were to completely melt away in all seasons, North Atlantic freshwater input would be about half this rate (see Box 4.1 for a discussion of observed and projected Arctic sea ice change). In all cases, the models exhibited a weakening of the AMOC (by a multimodel mean of 30% after 100 years), and none of the models simulated a shutdown. Ridley *et al.* (2005) elevated greenhouse gas levels to four times preindustrial values and retained them fixed thereafter to investigate the evolution of the Greenland Ice sheet in their coupled model. They found a peak melting rate of about 0.1 Sv, which occurred early in the simulation, and noted that this perturbation had little effect on the AMOC. Jungclaus *et al.* (2006) independently applied 0.09 Sv freshwater forcing along the boundary

---

Box 4.4. Would a Collapse of the AMOC Lead to Cooling of Europe and North America?

One of the motivations behind the study of abrupt change in the AMOC is its potential influence on the climates of North America and western Europe. Some reports, particularly in the media, have suggested that a shutdown of the AMOC in response to global warming could plunge western Europe and even North America into conditions much colder than our current climate. On the basis of our current understanding of the climate system, such a scenario appears very unlikely. On the multidecadal to century time scale, it is very likely that Europe and North America will warm in response to increasing greenhouse gases (although natural variability and regional shifts could lead to periods of decadal-scale cooling in some regions). A significant weakening of the AMOC in response to global warming would moderate that long-term warming trend. If a complete shutdown of the AMOC were to occur (viewed as very unlikely, as described in this assessment), the reduced ocean heat transport could lead to a net cooling of the ocean by several degrees in parts of the North Atlantic, and possibly 1 to 2 degrees Celsius over portions of extreme western and northwestern Europe. However, even in such an extreme (and very unlikely) scenario, a multidecadal to century-scale warming trend in response to increasing greenhouse gases would still be anticipated over most of North America, eastern and southern Europe, and Asia.

of Greenland as an upper-bound estimate of potential external freshwater forcing from the melting of the Greenland ice sheet. Under the SRES A1B scenario they, too, only found a weakening of the AMOC with a subsequent recovery in its strength. They concluded that Greenland ice sheet melting would not cause abrupt climate change in the 21st century.

Based on our analysis, we conclude that it is very likely that the strength of the AMOC will decrease over the course of the 21st century. Both weighted and unweighted multimodel ensemble averages under an SRES A1B future emission scenario suggest a best estimate of 25–30% reduction in the overall AMOC strength. Associated with this reduction is the possible cessation of LSW water formation. In models where the AMOC weakens, warming still occurs downstream over Europe due to the radiative forcing associated with increasing greenhouse gases (Gregory *et al.,* 2005; Stouffer *et al.,* 2006). No model under idealized (1%/year or 2%/year increase) or SRES scenario forcing exhibits an abrupt collapse of the AMOC during the 21st century, even accounting for estimates of accelerated Greenland ice sheet melting. We conclude that it is very unlikely that the AMOC will undergo an abrupt transition during the course of the 21st century. Based on available model simulations and sensitivity analyses, estimates of maximum Greenland ice sheet melting rates, and our understanding of mechanisms of abrupt climate change from the paleoclimate record, we further conclude it is unlikely that the AMOC will collapse beyond the end of the 21st century as a consequence of global warming, although the possibility cannot be entirely excluded.

8. WHAT ARE THE OBSERVATIONAL AND MODELING REQUIREMENTS NECESSARY TO UNDERSTAND THE OVERTURNING CIRCULATION AND EVALUATE FUTURE CHANGE?

It has been shown in this chapter that the AMOC plays a vital role in the climate system. In order to more confidently predict future changes—especially the possibility of abrupt change—we need to better understand the AMOC and the mechanisms governing its variability and sensitivity to forcing changes. Improved understanding of the AMOC comes at the interface between observational and theoretical studies. In that context, theories can be tested, oftentimes using numerical models, against the best available observational data. The observational data can come from the modern era or from proxy indicators of past climates.

We describe in this section a suite of activities that are necessary to increase our understanding of the AMOC and to more confidently predict its future behavior. While the activities are noted in separate categories, the true advances in understanding—leading to a predictive capability—come in the synthesis of the various activities described below, particularly in the synthesis of modeling and observational analyses.

8.1 Sustained Modern Observing System

We currently lack a long-term, sustained observing system for the AMOC. Without this in place, our ability to detect and predict future changes of the AMOC—and their impacts—is very limited. The RAPID project may be viewed as a prototype for such an observing system. The following set of activities is therefore needed:

- Research to delineate what would constitute an efficient, robust observational network for the AMOC. This could include studies in which model results are sampled according to differing observational networks, thereby evaluating the utility of those networks for observing the AMOC and guiding the development of new observational networks and the enhancement of existing observational networks.
- Sustained deployment over decades of the observational network identified above to robustly measure the AMOC. This would likely include observations of key processes involved in deep water formation in the Labrador and Norwegian Seas, and their communication with the rest of the Atlantic (*e.g.,* U.S. CLIVAR AMOC Planning Team, 2007).

We currently lack a long-term, sustained observing system for the AMOC.

• Focused observational programs as part of process studies to improve understanding of physical processes of importance to the AMOC, such as ocean-atmosphere coupling, mixing processes, and deep overflows. These should lead to improved representation of such processes in numerical models.

8.2 Acquisition and Interpretation of Paleoclimate Data

While the above stresses current observations, much can be learned from the study of ancient climates that provide insight into the past behavior of the AMOC. We need to develop paleoclimate datasets that allow robust, quantitative reconstructions of past ocean circulations and their climatic impacts. Therefore, the following set of activities is needed:

• Acquisition and analysis of high-resolution records from the Holocene that can provide insight on decadal to centennial time scales of AMOC-related climate variability. This is an important baseline against which to judge future change.
• Acquisition and analysis of paleoclimate records to document past changes in the AMOC, including both glacial and nonglacial conditions. These will provide a more robust measure of the response of the AMOC to changing radiative forcing and will allow new tests of models. Our confidence in predictions of future AMOC changes is enhanced to the extent that models faithfully simulate such past AMOC changes.
• More detailed assessment of the past relationship between AMOC and climate, especially the role of AMOC changes in abrupt climate change.
• Acquisition and analysis of paleoclimate records that can provide improved estimates of past changes in meltwater forcing. This information can lead to improved understanding of the AMOC response to freshwater input and can help to better constrain models.

8.3 Improvement and Use of Models

Models provide our best tools for predicting future changes in the AMOC and are an important pathway toward increasing our understanding of the AMOC, its variability, and its sensitivity

to change. Such insights are limited, however, by the fidelity of the models employed. There is an urgent need both to (1) improve the models we use and (2) use models in innovative ways to increase our understanding of the AMOC. Therefore, the following set of activities is needed:

• Development of models with increased resolution in order to more faithfully represent the small-scale processes that are important for the AMOC. The models used for the IPCC AR4 assessment had oceanic resolution on the order of 50–100 km in the horizontal, with 30–50 levels in the vertical. In reality, processes with spatial scales of several kilometers (or less) are important for the AMOC.
• Development of models with improved numerics and physics, especially those that appear to influence the AMOC. In particular, there is a need for improved representation of small-scale processes that significantly impact the AMOC. For example, overflows of dense water over sills in the North Atlantic are an important feature for the AMOC, and their representation in models needs to be improved.
• Development of advanced models of land-based ice sheets, and their incorporation in climate models. This is particulary crucial in light of uncertainties in the interaction between the AMOC and land-based ice sheets on long time scales.
• Design and execution of innovative numerical experiments in order to (1) shed light on the mechanisms governing variability and change of the AMOC, (2) estimate the inherent predictability of the AMOC, and (3) develop methods to realize that predictability. The use of multimodel ensembles is particularly important.
• Development and use of improved data assimilation systems for providing estimates of the current and past states of the AMOC, as well as initial conditions for prediction of the future evolution of the AMOC.
• Development of prototype prediction systems for the AMOC. These prediction systems will start from the observed state of the AMOC and use the best possible models, together with projections of future changes in

Models provide our best tools for predicting future changes in the AMOC and are an important pathway toward increasing our understanding of the AMOC, its variability, and its sensitivity to change.

atmospheric greenhouse gases and aerosols, to make the best possible projections for the future behavior of the AMOC. Such a prediction system could serve as a warning system for an abrupt change in the AMOC.

8.4 Projections of Future Changes in Radiative Forcing and Related Impacts

One of the motivating factors for the study of AMOC behavior is the possibility of abrupt change in the future driven by increasing greenhouse gas concentrations. In order to evaluate the likelihood of such an abrupt change, it is crucial to have available the best possible projections for future changes in radiative forcing, especially those changes in radiative forcing due to human activity. This includes not only greenhouse gases, which tend to be well mixed and long lived in the atmosphere, but also aerosols, which tend to be shorter lived

with more localized spatial patterns. Thus, realistic projections of aerosol concentrations and their climatic effects are crucial for AMOC projections.

One of the important controls on the AMOC is the freshwater flux into the Atlantic, including the inflow of freshwater from rivers surrounding the Arctic. For example, observations (Peterson *et al.,* 2002) have shown an increase during the 20th century of Eurasian river discharge into the Arctic. For the prediction of AMOC changes it is crucial to have complete observations of changes in the high-latitude hydrologic cycle, including precipitation, evaporation, and river discharge, as well as water released into the Atlantic from the Greenland ice sheet and from glaciers. This topic is discussed more extensively in Chapter 2.